UNIVERSIDADE DE SÃO PAULO
FACULDADE DE ODONTOLOGIA DE BAURU

MÁRCIA SIRLENE ZARDIN GRAEFF

# Osteoblastic response to biomaterials surfaces: mineralization evaluation and extracellular matrix proteomic analysis

# Resposta de osteoblastos a superfícies de biomateriais: avaliação da mineralização e análise proteômica da matriz extracelular

BAURU
2018

MÁRCIA SIRLENE ZARDIN GRAEFF

# Osteoblastic response to biomaterials surfaces: mineralization evaluation and extracellular matrix proteomic analysis

# Resposta de osteoblastos a superfícies de biomateriais: avaliação da mineralização e análise proteômica da matriz extracelular

Tese constituída por artigos apresentada a Faculdade de Odontologia de Bauru da Universidade de São Paulo para obtenção do título de Doutor em Ciências no Programa de Ciências Odontológicas Aplicadas, na área de concentração Estomatologia e Biologia Oral.
Orientador: Prof. Dr. Rodrigo Cardoso de Oliveira

**Versão Corrigida**

BAURU
2018

Graeff, Márcia Sirlene Zardin
Osteoblastic response to biomaterials surfaces: mineralization evaluation and extracellular matrix proteomic analysis / Márcia Sirlene Zardin Graeff. – Bauru, 2018.
85p. : il. ; 31cm.

Tese (Doutorado) – Faculdade de Odontologia de Bauru. Universidade de São Paulo

Orientador: Prof. Dr. Rodrigo Cardoso de Oliveira

**Nota**: A versão original desta tese encontra-se disponível no Serviço de Biblioteca e Documentação da Faculdade de Odontologia de Bauru – FOB/USP.

FOLHA DE APROVAÇÃO

**DEDICATÓRIA**

*Dedico este trabalho aos meus filhos Artur e Carlos. Ser a mãe de vocês sempre foi meu maior projeto.*

*Amo vocês infinitamente!*

## AGRADECIMENTOS

*Agradeço a Deus pelo dom da vida, que me foi concedida três vezes: ao nascer, ao me recuperar de um câncer de mama há dez anos, e ao descobrir e tratar um melanoma três anos atrás. Muito da minha vida mudou neste período, mas nunca a minha fé e a certeza da Sua Presença ao meu lado. Obrigada meu Deus por me possibilitar a realização de mais um sonho!*

*Aos meus pais, Derly (in memoriam) e Irede, que sempre me encorajaram a estudar e muito se esforçaram para que eu recebesse a melhor educação possível. Seus sonhos alcançaram um novo patamar hoje, com a primeira pessoa da família a concluir um Doutorado. Gratidão eterna!*

*Aos meus filhos Artur e Carlos, agradeço a oportunidade de me tornar uma pessoa melhor na vivência da maternidade. O amor a vocês me incentiva a seguir adiante, vencendo desafios. Sempre na certeza de que todo esforço e sacrifício valem a pena!*

*Aos meus irmãos Ciomara, Derly e Sabrina, que mesmo à distância estão sempre presentes, me apoiando em tudo. Amo muito!*

*Às minhas queridas Amigas do Peito, grupo de mulheres maravilhosas que me acolheram e ajudaram no momento mais difícil da minha vida. Vocês são a minha família em Bauru, obrigada por toda convivência e carinho! Um abraço especial à Clara, Cris e Meire, presentes na minha vida há dez anos com uma amizade inabalável!*

*Agradeço à Rafaela Alves, que além de ser colega de trabalho no CIP e na pós-graduação, se tornou uma grande amiga. Foram inúmeras vezes que você me ajudou, seja nos experimentos ou numa conversa tomando café. Muito obrigada por tudo!*

*Ao Marcelo Milanda, colega no CIP desde que cheguei em Bauru, meu muito obrigada! Foram tantas vezes que você me ajudou, com sua calma e prestatividade. Obrigada pela convivência harmoniosa e sua amizade!*

*À Cintia Tokuhara, minha fadinha querida! Sem você eu não teria conseguido desenvolver este trabalho! Você me ajudou com as células, com o planejamento dos experimentos, com as soluções e até me acompanhando e corrigindo no fluxo... Que você receba em dobro tudo que faz de bem pelos outros! Você tem minha gratidão, carinho e amizade para sempre!*

*À Mariana Liessa, uma flor de pessoa, que apesar da pouca convivência comigo se prontificou a me ajudar na preparação das amostras do proteoma, mesmo estando doente. Você foi uma heroína naquele dia! Gratidão!*

*Agradeço à Flavia Amadeu, que me ensinou sobre a cultura celular quando iniciei os pilotos deste trabalho. Sua competência e paciência são um exemplo para muitos! Muito obrigada!*

*À Adriana, Gabriela, e Mariana Santesso, que estão comigo desde que ingressei no grupo de pesquisa do Prof. Rodrigo. Tantas vezes me ajudaram, tirando dúvidas dos experimentos, materiais ou soluções. Muito obrigada mesmo! E aos outros colegas do grupo, agradeço a oportunidade de conviver e trocar ideias. Desejo muito sucesso a todos vocês!*

*Agradeço também a amizade e carinho da Priscila, com quem convivi tanto tempo no confocal. Admiro sua dedicação e competência! Meu agradecimento também à Aline, Daiana e Juliana, e aos outros colegas do Laboratório de Bioquímica, pela parceria e boa convivência.*

*Agradeço aos usuários do CIP e principalmente do confocal (impossível nomear todos), pela convivência agradável, conversas e risadas que temos no dia-a-dia, que muito me alegram. Adoro meu trabalho e todos vocês fazem parte da minha vida de maneira especial!*

*À Mileni Fernandes, pela capacidade técnica e prestatividade ao realizar a análise no espectrômetro de massas. Muito obrigada pela sua ajuda, sem a qual não teria sido possível finalizar este projeto!*

*Ao Prof. Dr. Luis Augusto Rocha, da Unesp Bauru, pela parceria neste trabalho desde o início. Além de nos ceder amostras de titânio puro e anodizado, as ricas discussões que tivemos sobre o projeto foram de grande valia. Muito obrigada!!*

*Ao Prof. Dr. Diego Rafael Nespeque Correa, pela ajuda com o lote final das amostras de titânio anodizado e por me ensinar sobre o processo de anodização. Muito obrigada!*

*À Thelma, especialista em laboratório do Departamento de Bioquímica, pela ajuda com os reagentes e principalmente pela amizade sincera. Um grande abraço!*

*À Dalva, secretária de pós-graduação da Biologia Oral, por toda orientação recebida e pela amizade. Às secretárias da Pós-graduação Fátima, Ana Letícia e Leila, pelo suporte aos nossos trabalhos.*

*Agradeço à Faculdade de Odontologia de Bauru-USP, na pessoa do diretor Prof. Dr. Carlos Ferreira dos Santos, e da senhora Presidente da Comissão de Pós-Graduação Profa. Dra. Izabel Regina Fischer Rubira de Bullen, pela oportunidade de aprendizado.*

## AGRADECIMENTO ESPECIAL

*Agradeço em especial ao meu orientador Prof. Dr. Rodrigo Cardoso de Oliveira, que acreditou em minha capacidade e aceitou minha ideia de um projeto de Doutorado avaliando biomateriais com microscopia confocal.*

*Pouco tempo depois, além de meu orientador, tive a sorte de tê-lo também como chefe, quando assumiu a Coordenação do CIP.*

*Desde o início, você não poupou esforços para conseguir condições de desenvolver este trabalho, mesmo sem a ajuda direta de agências de fomento. Sempre pude contar com sua experiência e paciência. Admiro sua organização e cuidado com todos os seus alunos.*

*Muito obrigada por tudo!!*

*"Volta teu rosto sempre na direção do sol e,*
*então, as sombras ficarão para trás."*
*(Provérbio chinês)*

## ABSTRACT

**Osteoblastic response to biomaterials surfaces: mineralization evaluation and extracellular matrix proteomic analysis**

Dental implants are designed to replace tooth loss, due to periodontal diseases, trauma or decay. Among the biomaterials used for this purpose, titanium and zirconia have been investigated for some years, with excellent mechanical properties and biocompatibility. Surface treatments such as anodizing, with the incorporation of Mg, Ca and P in the structure of the titanium oxide films, were used in order to increase tribocorrosion resistance and improve the osseointegration process. The cellular response to surfaces is mediated, among other factors, by the extracellular matrix (ECM) . However, very little is still known about the ECM proteomics during mineralization. Our objective was a longitudinal comparison of osteoblastic behavior on different materials, in terms of mineralization volume and actin cytoskeleton status, associated with the proteomic analysis of the extracellular matrix. The three types of biomaterial surfaces (pure titanium, anodized titanium and zirconia) were imaged by confocal 3D microscopy and analyzed in terms of roughness. MC3T3 cells were cultivated on the biomaterials for 7, 14 and 21 days, with osteogenic medium containing calcein. The cells were then fixed, stained with Rhodamine phalloidin and DAPI, and imaged by confocal laser scanning microscopy. The quantification of mineralization and actin cytoskeleton was performed by a novel technique, based on the acquired 3D images. For the proteomic analysis, the specimens were washed, decellularized and the ECM was collected in buffer solution. The anodized titanium surface is more porous when compared to that of cp-Ti and zirconia, and superior mineralization was obtained over it after 21 days of culture. The actin microtubular volume was increased on the three materials on the first 14 days, but on the 21th day there was a reduction over anodized titanium and zirconia, related to mineralization phase.. Conclusion: The greater mineralization obtained over anodized titanium after 21 days demonstrated an improved response provided by the surface modification. The innovative volume quantification technique adopted was useful in providing information about the cellular status and biomaterial performance. Alpha-1_4 glucan phosphorylase and Glycogen phosphorylase brain form were down-regulated on

zirconia after 7 and 14 days of culture, and up-regulated on Anod Ti on the 7$^{th}$ day, suggesting the influence of material surface roughness and chemical composition on energy metabolism. Proteins related to bone development, like TGF-β3, were found exclusively on cp-Ti on the 21$^{st}$ day. The small number of identified proteins demonstrates that the chosen decellularization process was effective at reducing the proteome dataset. Altogether, our results reveal new insights regarding osseointegration and how material surfaces affect this process.

**Key words:** Osteoblasts. Biomaterials. Bone Mineralization. Extracellular matrix. Proteomics.

**RESUMO**

## Resposta de osteoblastos a superfícies de biomateriais: avaliação da mineralização e análise proteômica da matriz extracelular

Implantes dentários são projetados para substituir a perda de dentes, que pode ser causada por doenças periodontais, traumas ou cáries. Entre os biomateriais utilizados para este fim, titânio e zircônia têm sido investigados durante alguns anos, com excelentes propriedades mecânicas e biocompatibilidade. Tratamentos de superfície como a anodização, com a incorporação de Mg, Ca e P na estrutura dos filmes de óxido de titânio, foram utilizados a fim de aumentar a resistência à tribocorrosão e melhorar o processo de osseointegração. A resposta celular às superfícies é mediada, entre outros fatores, pela matriz extracelular (ECM). No entanto, muito pouco ainda é conhecido sobre a proteômica da matriz óssea durante a mineralização. Nosso objetivo foi a comparação longitudinal do desempenho de osteoblastos em diferentes materiais em termos do volume da mineralização e do status do citoesqueleto de actina, associada à análise proteômica da matriz extracelular. Imagens dos três tipos de superfícies de biomateriais (titânio puro, titânio anodizado e zircônia) foram adquiridas por microscopia confocal 3D e analisadas em termos de rugosidade. Células MC3T3 foram cultivadas na superfície dos biomateriais durante 7, 14 e 21 dias, com meio osteogênico contendo calceína. As células foram então fixadas, coradas com faloidina-rodamina e DAPI, e levadas ao microscópio confocal de varredura a laser. A quantificação da mineralização e do citoesqueleto de actina foi feita por uma nova técnica, baseada em imagens 3D. Para a análise proteômica, os espécimes foram lavados, descelularizados e a matriz extracelular foi coletada em solução tampão. A superfície de titânio anodizado é mais porosa quando comparada com a de cp-Ti e zirconia e apresentou mineralização superior após 21 dias de cultura. O volume dos microtúbulos de actina foi aumentado sobre os três materiais nos primeiros 14 dias, mas no 21º dia houve uma redução relacionada ao aumento da mineralização sobre o titânio anodizado e zirconia. Conclusão: a mineralização superior obtida sobre o titânio anodizado após 21 dias de cultura demonstrou a melhoria provocada pela modificação de superfície. A nova técnica adotada para a quantificação do volume foi útil para fornecer informações sobre o status celular e o

desempenho dos biomateriais. Alpha-1_4 glucano fosforilase e glicogênio fosforilase forma cerebral foram sub-expressas sobre a zircônia após 7 e 14 dias de cultura e sobre-expressas sobre o titânio anodizado no 7º dia, sugerindo a influência da rugosidade e composição química da superfície dos materiais no metabolismo de energia. Algumas proteínas relacionadas com o desenvolvimento ósseo, como a TGF-β3, foram encontradas exclusivamente sobre o cp-Ti no 21º dia. A pequena quantidade de proteínas identificadas demonstra que o processo de descelularização adotado foi eficiente em reduzir o conjunto de dados da análise proteômica. Em suma, nossos resultados revelam novos detalhes sobre a osseointegração e como a superfície dos materiais podem afetar esse processo.

**Palavras-chave:** Osteoblastos. Biomateriais. Mineralização óssea. Matriz extracelular. Proteoma.

## TABLE OF CONTENTS

# 1 Introduction

# 1 INTRODUCTION

Dental implants are designed to replace tooth loss, which can be caused by periodontal diseases, trauma, or decay. Among the biomaterials used for this purpose, titanium is the most commonly used. Its biocompatibility and mechanical properties have been proved excellent over more than 50 years. However, all metal implants are subjected to gradual degradation when placed in contact with the electrolytic environment of the human body (1). Degradation may occur by electrochemical corrosion, often together with mechanical wear caused by micromovements induced by mastication (2). As a consequence, an increase of metallic ions and/or nanometric metallic-based particles may reach the circulatory system and accumulate in other organs (2). Besides, particles may be stored locally in the gingival tissue surrounding the implant, causing inflammation and undesirable color changes (3).

Superior tribocorrosion performance for metal implants can be achieved by surface modifications. Changes in composition, morphology or structure can be made, while keeping the substrate mechanical properties. Anodizing treatments has been widely used on this purpose, providing better hard tissue compatibility and accelerating bone formation over implants (1). Indispensable elements in bone formation, Ca and P ions may be incorporated on the deposited layer, leading to better tribocorrosion resistance (4). Besides cellular behaviors such as adhesion, spreading and IFN-γ cytokine secretion are affected , which may lead to shorter rehabilitation times (5)

Ceramic implants pose an alternative to avoid corrosion issues related to metallic counterparts. A review article by Hisbergues (2008) emphasized zirconia properties like resistance to corrosion and aesthetic appeal, as well as the fact that healthier gum tissue is developed around ceramic implants (6). The grey color of the titanium implants may become visible when placed to restore anterior teeth, especially in cases of thin gingival tissue (3). More research is needed over the long-term performance of zirconia implants, as its use in dental clinic is recent (3,7–9).

The major factor impacting the long-lasting performance of an implant is the osseointegration, which is the capacity of building new bone around it. This characteristic may be evaluated by the amount of mineralization obtained when bone cells are cultivated over the material (10).

Short-term responses such as cell number and alkaline phosphatase expression do not necessarily correspond to greater mineralization. Aiming to analyze calcified nodules directly, Ahmad et al. (1999) introduced fluorescent marking by calcein, in a study comparing Tivanium and Zimaloy with glass, as substrates for a 6-weeks long osteoblastic culture (11).

In another study on mineralization obtained over titanium, de Oliveira et al. (2007) demonstrated that a chemically caused nanotopography on the titanium surface improved the osteoblastic response, possibly due, between other factors, to the fact that the modified surface is more hydrophilic than the untreated surface (12).

Hempel et al (2010) compared the cellular response caused by two surface treatments on titanium and zirconia. The osteoblasts grown on the zirconia showed greater accumulation of calcium in the mineral nodules than those grown on titanium. There was little difference between the treated and untreated zirconia surface (13).

Several processes are triggered when osteoblasts meet a surface, leading to adhesion, proliferation and differentiation, many of them mediated by the cytoskeleton. Besides, cell morphology is determined by the cytoskeleton, which is known to change during the osteoblastic mineralization process (14).

Confocal laser scanning microscopy (CLSM) has been largely used to analyze cell morphology, structures and functions. Its ability to provide high resolution and high contrast 3D image stacks allow feasible and trustworthy volume measurements. Additionally, fluorescent labelling of intracellular proteins or organelles have been proven specific and reliable (15). Kihara et al. (2004) used CLSM to visualize calcein-stained mineralization nodules and compared them with conventional Alizarin staining, confirming the quantitative correlation between calcein deposition and calcium contents (16). However, the CLSM images were used to quantify the fluorescent intensity, not the nodular size. The use of confocal volume quantification to measure the amount of mineralization obtained by cultured osteoblasts has not yet been described in the biomedical literature.

Cellular responses to material surfaces are determinant for a successful implant performance. After adhering, proliferating and spreading over the implant surfaces, it is mandatory for the osteoblasts to be able to generate bone around the implant, a process called osseointegration, which guarantees the long-term stability of the implant (14).

Bone formation is a not fully understood process, which involves mineralization of the extracellular matrix by the deposition of hydroxyapatite, rich in calcium and other minerals. The extracellular matrix (ECM) provides structural support for the cells within a tissue, besides directing important events such as cell proliferation, survival, differentiation, and migration. Composed of water, collagens, glycoproteins and proteoglycans, the ECM is a complex structure that is constantly being remodeled (17). Grzesiak et al. (2017) concluded that ECM synthesis and mineral deposition during the osteogenic differentiation involves cell death and mineralization nodules derive from calcium rich cellular remnants (18).

The field of proteomics has contributed to the understanding of many cellular processes. Still, very little is known about the ECM proteomics during mineralization. The protein profiles of the ECM and matrix vesicles (MVs) of mineralizing osteoblasts was described for the first time in the work of Xiao et al. (2007). The cells were cultivated on conventional culture plates, and the cellular content was separated from the ECM proteins by gel electrophoresis. However, this work had no relation to biomaterials interaction (19).

Comparison of the whole proteomic profile of human osteoblasts grown over two biomaterials was conducted by Jinling Xu (2008), but only for an initial phase (4 days of incubation) (20). A description of the protein content of an isolated ECM was presented by Rashid et al. (2012) using an *in vitro* model of fibrotic liver tissue, where the samples were decellularized (21). This interesting approach directs the proteomic analysis to a focused dataset.

Many efforts have been undertaken towards elucidating cell attachment and proliferation over biomaterials, but less work has been done investigating the effect the surface properties can exert on the late steps of osseointegration, such as the mineralization phase. Our objective was to compare, in a longitudinal manner, the cellular response to anodized titanium (Anod Ti) and yttria stabilized zirconia (Y-TZP) with that obtained over commercially pure titanium (cp-Ti) by 1) measuring the mineralization and actin cytoskeleton volumes, based on 3D confocal microscopy; and 2) analyze the proteome of the decellularized ECM, by mass spectrometry. It will certainly contribute to elucidate the influence of biomaterials surfaces on the process of osseointegration.

*2 Articles*

## 2 ARTICLES

This thesis was divided in two articles, written in accordance to *JAOS* and *Bone* Guidelines, respectively:

• ARTICLE 1 – On a novel method for evaluation of the mineralization process of osteoblasts on biomaterials surfaces.

• ARTICLE 2 – Longitudinal comparison of the ECM proteins from osteoblasts cultivated on different biomaterials.

## 2.1 **ARTICLE 1**

### On a novel method for evaluation of mineralization process of osteoblasts on biomaterials surfaces

Graeff MSZ[1], Tokuhara CK[2], Oliveira RC [1,2,3]

1 Centro Integrado de Pesquisas CIP 1 Faculdade de Odontologia de Bauru- FOB/USP

2 Departamento de Ciências Biológicas, Faculdade de Odontologia de Bauru- FOB/USP

3 Braço Brasileiro do Instituto de Biomateriais, Tribocorrosão e Nanomedicina (IBTN/Br)

***Corresponding author**:

Prof. Dr. Rodrigo Cardoso de Oliveira

Department of Biological Sciences - Bauru School of Dentistry/ University of São Paulo

Al. Dr. Octavio Pinheiro Brisolla, 9-75, Vila Universitária, Bauru/SP, Zip Code: 17012-901, Bauru,SP, Brazil.

E-mail Address: rodrigocardoso@usp.br

Phone: 55 14 32358247 and 55 14 32358321

**Abstract**

Dental implants are designed to replace teeth lost due to periodontal diseases, trauma, or decay. Among the biomaterials used for this purpose, titanium and zirconia have been investigated for some years, with excellent mechanical properties and biocompatibility. In order to improve the osseointegration process and increase durability, surface treatments like anodization have been used on titanium. Our objective was to compare anodized commercially pure titanium with only etched surfaces and yttria-stabilized zirconia (Y-TZP) in terms of mineralization volume and cellular morphology status, using a novel quantification method. The three biomaterial surfaces were imaged by 3D confocal microscopy and analyzed in terms of roughness. MC3T3 cells were cultured on biomaterials surface for 7, 14 and 21 days. Afterwards, the cells were fixed and labeled with Rhodamine phalloidin and DAPI. The 3D image stacks were acquired on a Leica TCS SPE Confocal Laser Scanning Microscope. Actin cytoskeleton and nodular mineralization volumes were measured by software. The anodized titanium surface is more porous compared to cp-Ti and Y-TZP and presented superior mineralization after 21 days of culture. The actin microtubular volume was increased on the three materials on the first 14 days, but over anodized titanium and zirconia it was reduced on the 21th day, due to the morphological change associated with the mineralization phase. Conclusion: The major mineralization obtained over anodized titanium after 21 days of culture demonstrated an improved response provided by the surface modification. The volume quantification technique adopted was useful in providing information about the cellular status and mineralization.

**Key words:** Osteoblasts. Biomaterials. Bone Mineralization. Confocal Microscopy.

**Introduction**

Dental implants are designed to replace teeth that were lost due to periodontal diseases, trauma, or decay. Among the biomaterials used to build dental implants, titanium is the most commonly used. Its biocompatibility and mechanical properties have proved to be adequate over more than 50 years. However, all metallic implants are subjected to gradual degradation when placed in contact with the electrolytic environment of the human body (1). Degradation may occur by electrochemical corrosion, often together with mechanical wear caused by micromovements induced by mastication (2). As a consequence, metallic ions and/or nanometric metallic-based particles may reach the circulatory system and accumulate in other organs (3). Besides, particles may be stored locally in the gingival tissue surrounding the implant, causing inflammation and undesirable color changes (4).

Superior tribocorrosion performance for metallic implants can be achieved by surface modifications. Changes in surface composition, morphology or structure can be engineered, while keeping the substrate mechanical properties. Anodizing treatments have been widely used for this purpose, providing better hard tissue compatibility and accelerating bone formation over implants (1). The incorporation of Ca and P ions on the deposited layer affects the cellular behavior such as proliferation, differentiation and gene expression, being an excellent choice (5,6).

A review article by Hisbergues (2008) emphasized zirconia properties like resistance to corrosion and aesthetic appeal, as well as the fact that healthier gum tissue is developed around ceramic implants (7). The grey color of titanium implants may become visible when placed to restore anterior teeth, especially in cases of thin gingival tissue (4). More research is needed on the long-term performance of zirconia implants, since its use in dental clinic is recent (4,8–10).

The major factor impacting the long-lasting performance of an implant is osseointegration, which is the capacity of building new bone around it. This characteristic can be evaluated by the amount of mineralization obtained when bone cells are cultured over the material (11).

Several processes are triggered when osteoblasts meet a surface, leading to adhesion, proliferation and differentiation, many of them mediated by the cytoskeleton. Besides, cell morphology is determined by the cytoskeleton, which is known to change during the osteoblastic mineralization process (12).

Confocal laser scanning microscopy (CLSM) has been largely used to analyze cell morphology, structures and functions. Its ability to provide high resolution and high contrast 3D image stacks allow feasible and trustworthy volume measurements. Additionally, fluorescent labelling of intracellular proteins or organelles have been proven specific and reliable (13). Kihara et al. (2004) used CLSM to visualize calcein-stained mineralization nodules and compared them with conventional Alizarin staining, confirming the quantitative correlation between calcein deposition and calcium contents (14). However, the CLSM images were used to quantify the fluorescent intensity, not the nodular size. The use of confocal volume quantification to measure the amount of mineralization obtained by cultured osteoblasts has not yet been described in the biomedical literature.

Many efforts have been undertaken to elucidate the cell attachment and proliferation over biomaterials, but less work has been done to investigate the effect of surface properties on the late steps of osseointegration, such as the mineralization phase. Our objective was to compare the cellular response to anodized titanium surface with commercially pure titanium (cp-Ti grade 2) and yttria-stabilized zirconia (Y-TZP) by measuring the mineralization and actin cytoskeleton volumes, using a novel method, based on 3D confocal microscopy.

## Material and Methods

*Sample preparation*

All samples were equal in size, namely 10 x 10 x 2 mm squares. Commercially pure titanium grade 2 (cp-Ti) was used as control group and the bulk material for the anodization process, as described in the work of Ribeiro et al (2015) (5). The cp-Ti specimens were etched individually in a solution containing nitric acid ($HNO_3$), hydrofluoric acid (HF) and distilled water in equal proportions (1:1:1) for 15 seconds to remove the native oxide layer. This process was followed by a bath in ethyl alcohol with ultrasound for 15 min and drying in an oven.

For the anodic treatment, a solution of 0.02M β-glycerophosphate disodium salt pentahydrate, 0.35M calcium acetate monohydrate and 0.1 M magnesium acetate monohydrate was used. Anodization was carried out for 1 min at a constant voltage of 300 V, using a platinum rod as the counter electrode, under magnetic agitation. The anodized samples were taken to a drying oven for 4 hours. This group was named Anod Ti.

The IPS e.max ZirCAD yttria-stabilized zirconia block from Ivoclar Vivadent was cut into 12.5 x 12.5 x 3.0 mm square pieces, and then ground with silicon carbide sandpaper (600 grit). Sintering was conducted in an inFire HTC Speed (Sirona) oven, as indicated by the supplier. The final size was 10 x 10 x 2 mm. Afterwards, the zirconia samples were washed with detergent under running water, cleaned by sonication in deionized water for 10 min and dried with hot air blow.

Prior to cell culture, all samples were autoclaved for 15 min at 120°C and dried overnight in a drying oven.

*Surface Analysis*

Using 3D confocal microscopy, randomly selected samples of the three biomaterials were imaged and analyzed in terms of roughness. A Leica DCM 3D (Leica Microsystems, Mannheim) microscope was used, with a 50x/0.9 objective. Six fields were imaged on each sample, separated by 1 mm in x and y directions. Three samples of each biomaterial were analyzed. The area of each field was 254.64 x 190.90 µm, with a z step size of 0.2 µm. The software Leica MAP v.6.2.7200 was used to quantify the average area roughness (Sa). Besides, the samples were examined by backscattered scanning electron microscopy, using a JEOL JSM-7400F microscope operated at 30 kV, with a final magnification of 2500x.

*Cell culture*

Murine preosteoblastic MC3T3 cells (ATCC® CRL-2593™)(15), passage number 13, were cultured for 7, 14 and 21 days, in modified osteogenic media. ’ Basically, α-MEM media supplemented with 10% BFS, 50 µg.mL-1 acid ascorbic and 10 mM β-glycerophosphate (Sigma®) was used (16). The addition of 1µg/mL of calcein (known to bind to Ca ions) to the osteogenic media followed the protocol established by Kihara et al. (2004) (14), for green fluorescent labelling of mineralization nodules. Cells were plated at a density of $10^4$ cells per

well. Half of the medium was changed every third day. Afterwards, the cells were fixed with paraformaldehyde (2% in PBS, 20 min, 37°C) and washed three times with PBS. Rhodamine phalloidin, a high-affinity F-actin probe conjugated to the red-orange fluorescent dye, tetramethylrhodamine (TRITC), was used to label the actin cytoskeleton, as indicated by the supplier (Invitrogen™). The samples were mounted face up on glass slides and covered with round 13mm coverslips. ProLong™ Diamond Antifade Mountant with DAPI (Invitrogen™) was used to counterstain nuclei in blue.

The 3D image stacks were acquired on a Leica TCS SPE Confocal Laser Scanning Microscope, using a 40x/1.15 oil objective. On each sample, six fields of 275 X 275 µm were imaged, with a z step size of 1µm. The mineralization and actin microtubular volumes were measured by Leica LAS X software. Using Statistica software, two-way Anova followed by Fischer´s LSD were run to evaluate the effects of culture times and substrate types on mineralization and actin cytoskeleton volumes. Besides, Pearson's correlation coefficient was calculated.

**Results**

*Surface Analysis*

Figure 1 shows representative images of each biomaterial acquired by 3D confocal microscopy and scanning electron microscopy. The Leica MAP analysis software was used to generate the 3D surface reconstructions, as well as the topographic images, where surface heights are color-coded. Within each group, the samples were very similar in terms of topography, morphology and roughness. The cp-Ti surface presented a granular microstructure and its average area roughness (Sa) was 2.6 ±0.552 µm. The Anod Ti surface showed a porous structure with a Sa about 2.1 ±0.464 µm. The zirconia surface was flat, smooth, and very uniform; therefore, its average roughness was much smaller, namely 0.4 ±0.079 µm (Figures 1 and 2).

*Cell culture*

Representative micrographs of the osteoblasts morphology of each group according to the culture time can be seen in figure 3. The increasing number of cells in all groups can be evaluated qualitatively by the number of blue labelled cell nuclei. The mineralization process began only after 14 days of culture, as revealed by the calcein green fluorescence. At first, just few spots of mineral deposition were seen, which became denser and accumulated by the 21th culture day. The red actin filaments show the cellular morphology, which was initially spread and flat, with strong stress fibers. Later the cells became less flat, with fewer and thinner actin filaments, suggestive of a cuboid phase.

Regarding the mineralization volume quantified (Figure 4), the amount of mineralization was increased over time for all groups. There was no significant difference between materials after 7 and 14 days of culture. After 21 days, the amount of mineralization was equivalent between cp-Ti and zirconia. The anodized Ti surface exhibited the greatest mineralization volume in comparison to other biomaterials. As the absolute values were much greater after 21 days of culture in comparison with earlier times, logarithmic scale was used for the y axis.

After 7 and 14 days of culture, the actin microtubular volume was increasing on the three biomaterials, with no difference between groups (Figure 5). On the 21th day, there was a reduction over anodized Ti surface and zirconia, while still increasing over cp-Ti, where the actin cytoskeleton volume was much bigger.

There was a weak inverse correlation between mineralization and actin cytoskeleton volume in all groups, at all times considered. A downhill (negative) linear relationship, with $r=-0.21$ and $p=0.002$, was obtained for the whole data set.

**Discussion**

Dental implant failures cause patient discomfort and bone loss is often clinically observed. It is therefore important to assure good osseointegration ability and appropriate mechanical properties to withstand the masticatory pressures. Alternatives for clinical choice beyond commercially pure titanium should be presented. Titanium is the gold standard for dental implant industry, but new materials as well as surface treatments have been investigated aiming at a long-lasting performance allied to improved aesthetics. In this context, we decided to compare three different biomaterials: commercially pure titanium (cp-Ti grade 2), anodized titanium surface and yttria-stabilized zirconia (Y-TZP), in a longitudinal study.

Zirconia needs to be stabilized to achieve ideal mechanical properties (7,17). Yttria-stabilized tetragonal zirconia polycrystal (Y-TZP) is the most frequently used material for ceramic oral implants (18). However, controversial results have been achieved, and no final decision has been established about its use in the clinic (10).

Surface treatments like polishing, sandblasting, acid etching, coatings, nanotextures and biofunctionalization have been proposed and tested over titanium and zirconia (18–23). As mentioned earlier, the anodization process improves cell attachment and proliferation (24), but less work has been done on the final steps of osseointegration and the bone quality obtained. Techniques used to evaluate mineralization include von Kossa staining (25), colorimetric assays based on alizarin red staining (26), or EDX (27). Direct fluorescent labelling of hydroxyapatite crystals by calcein was used for visualization (14,28), fluorometric quantitation (11,29) or nodule area measurement (20,30), but no work has been published measuring the mineralization volume based upon confocal 3D imaging.

Colorimetric or fluorometric quantification methods rely on chemical reactions to solubilize the product being investigated. These reactions might be incomplete, and therefore inaccurate. Although fast, there is no information on how the substance is distributed over the sample, while imaging-based quantification methods allow visualization. Standard microscopy methods are based on two-dimensional projections of real objects on the camera plane, while in laser scanning methods the images are built point by point, also in the z axis. Confocal microscopy offers better contrast and resolution, and despite being slower, it provides means for precise three-dimensional measurements (13).

When comparing anodized titanium (TiUnite®), machined titanium (Ti-m), sandblasted and acid-etched zirconia (TZP- proc), and machined zirconia (TZP-A-m), Kohal et al. (2013) (18) observed contradictory results. Similar to our results, the cell responses to zirconia surfaces were comparable to those obtained over titanium, but in the *in vivo* experiment TZP-proc performed worse than a standard titanium implant surface modification. Hempel et al. (2010) also compared titanium and zirconia with two surface modifications, and significantly higher calcium accumulation was obtained on both zirconia surfaces when compared with titanium (31).

In our work, cp-Ti was the roughest surface, while zirconia was the smoothest. Notwithstanding, the amount of mineralization obtained over both materials was equivalent. Our results suggest that roughness alone may not be a determining parameter concerning cell behavior, agreeing with the conclusion presented by Setzer et al in 2008 (26). Besides, this result strengthens the use of zirconia in the clinic by suggesting that both materials would present a similar osseointegration. On the other hand, anodized titanium presented a greater mineralization volume compared to the other two biomaterials, probably due to its chemical composition or porosity, as suggested in the works of Alves et al. (21,32). Also, Anselme et al. (33) (2000) stated that there was a negative correlation between roughness and cell adhesion and proliferation, yet the roughness organization and surface chemical composition were relevant, as it seems to be the case for anodized titanium in our work.

In the present study, all biomaterials showed a good proliferation of MC3T3 cells. It has been reported that osteoblasts undergo shape changes as they differentiate: the cell loses its flattened, elongated shape and adopts a cuboidal morphology. The actin restructuring observed after 14 days of culture is in agreement with the results shown in previous studies by Titushkin et al (2007) (34) and Meng et al (2009) (35).

Among many other functions like adhesion (36), migration and cellular morphology, the cytoskeleton is responsible for vesicle transport. Osteoblasts release matrix vesicles (MVs), which are the initial sites where crystals of apatite bone mineral are formed (37).

Recently, many efforts have been undertaken to understand the process and mechanism of MV formation and release. Some results have suggested that the MV release is mediated by

the actin cytoskeleton. A correlation between the release of MVs and changes in cellular actin distribution has been reported by Hale and colleagues (38). Furthermore, actin microfilament disassembly is involved in the mechanism of MV formation, as Thouverey and colleagues demonstrated (39).

Our current data have shown a weak inverse correlation between mineralization and actin cytoskeleton volumes, reinforcing the role of actin fibers depolymerization in the formation of MVs. According to this result, it may be interesting to investigate other techniques like fluorescent colocalization or proteomics to further elucidate this mechanism.

## Conclusions

The greater mineralization obtained over anodized titanium after 21 days demonstrated an improved response provided by the surface modification. The amount of mineral deposition obtained over zirconia was equivalent to that of cp-Ti, which favors the use of zirconia in the clinic. An inverse correlation between mineralization and cytoskeleton volume has been shown, strengthening the hypothesis of actin fibers depolymerization related to mineral deposits through MVs. The innovative volume quantification technique adopted was useful in providing information about the cellular status and biomaterial performance in terms of osseointegration.

## Acknowledgments

The authors thank Heitor Marques Honório for assistance in statistical analysis and Centro Integrado de Pesquisa (CIP), Bauru School of Dentistry, USP for providing research facilities. Special thanks to Prof. Dr. Luís Augusto Rocha, Departamento de Física, Faculdade de Ciências - FC/UNESP Bauru, for the donation of the commercially pure and anodized titanium samples.

## References

1. Alves a C, Oliveira F, Wenger F, Ponthiaux P, Celis J-P, Rocha L a. Tribocorrosion behaviour of anodic treated titanium surfaces intended for dental implants. J Phys D Appl Phys [Internet]. 2013 Oct 9;46(40):404001. Available from: http://stacks.iop.org/0022-3727/46/i=40/a=404001?key=crossref.798810ece9bd05ce3c9a76ad76114463
2. Mathew MT, Abbey S, Hallab NJ, Hall DJ, Sukotjo C, Wimmer MA. Influence of pH on the tribocorrosion behavior of CpTi in the oral environment: synergistic interactions of

wear and corrosion. J Biomed Mater Res Part B Appl Biomater [Internet]. 2012 Aug;100B(6):1662–71. Available from: http://doi.wiley.com/10.1002/jbm.b.32735

3. Ribeiro AR, Gemini-Piperni S, Travassos R, Lemgruber L, Silva RC, Rossi AL, et al. Trojan-Like Internalization of Anatase Titanium Dioxide Nanoparticles by Human Osteoblast Cells. Sci Rep [Internet]. 2016 Mar 29 [cited 2017 Jan 20];6:23615. Available from: http://www.nature.com/articles/srep23615
4. Özkurt Z, Kazazoğlu E. Zirconia dental implants: a literature review. J Oral Implantol [Internet]. 2011 Jun [cited 2014 Feb 4];37(3):367–76. Available from: http://www.ncbi.nlm.nih.gov/pubmed/20545529
5. Ribeiro AR, Oliveira F, Boldrini LC, Leite PE, Falagan-Lotsch P, Linhares ABR, et al. Micro-arc oxidation as a tool to develop multifunctional calcium-rich surfaces for dental implant applications. Mater Sci Eng C. 2015;54:196–206.
6. Oliveira FG, Ribeiro AR, Perez G, Archanjo BS, Gouvea CP, Araújo JR, et al. Understanding growth mechanisms and tribocorrosion behaviour of porous TiO2 anodic films containing calcium, phosphorous and magnesium. Appl Surf Sci. 2015;341:1–12.
7. Hisbergues M, Vendeville S, Vendeville P. Zirconia: Established facts and perspectives for a biomaterial in dental implantology. J Biomed Mater Res B Appl Biomater [Internet]. 2009 Mar [cited 2014 Jan 31];88(2):519–29. Available from: http://www.ncbi.nlm.nih.gov/pubmed/18561291
8. Soon G, Pingguan-Murphy B, Lai KW, Akbar SA. Review of zirconia-based bioceramic: Surface modification and cellular response. Vol. 42, Ceramics International. 2016. p. 12543–55.
9. Assal P. The Osseointegration of Zirconia Dental Implants. … fur Zahnmedizin= Rev Mens suisse d'odonto- … [Internet]. 2012 [cited 2014 Feb 4]; Available from: http://europepmc.org/abstract/MED/23965893
10. Martins R, Cestari TM, Arantes RVN, Santos PS, Taga R, Carbonari MJ, et al. Osseointegration of zirconia and titanium implants in a rabbit tibiae model evaluated by microtomography, histomorphometry and fluorochrome labeling analyses. J Periodontal Res. 2018;53(2):210–21.
11. Uchimura E, Machida H, Kotobuki N, Kihara T, Kitamura S, Ikeuchi M, et al. In-situ visualization and quantification of mineralization of cultured osteogenetic cells. Calcif Tissue Int [Internet]. 2003 Dec [cited 2014 Jan 4];73(6):575–83. Available from: http://www.ncbi.nlm.nih.gov/pubmed/12958691
12. Meyer U, Büchter A, Wiesmann HP, Joos U, Jones DB. Basic reactions of osteoblasts on structured material surfaces. Eur Cell Mater. 2005;9:39–49.
13. Lee K, Yeung H. Application of Laser Scanning Confocal Microscopy in

Musculoskeletal Research. In: Advanced Bioimaging Technologies in Assessment of the Quality of Bone and Scaffold Materials [Internet]. Berlin, Heidelberg: Springer Berlin Heidelberg; p. 173–89. Available from: http://link.springer.com/10.1007/978-3-540-45456-4_10

14. Kihara T, Oshima A, Hirose M, Ohgushi H. Three-dimensional visualization analysis of in vitro cultured bone fabricated by rat marrow mesenchymal stem cells. Biochem Biophys Res Commun [Internet]. 2004 Apr 9 [cited 2014 Jan 4];316(3):943–8. Available from: http://www.ncbi.nlm.nih.gov/pubmed/15033493
15. H. Sudo, H. A. Kodama, Y. Amagai, S. Yamamoto SK. In Vitro Differentiation and Calcification in a New Clonal Osteogenic Cell Line Derived from Newborn Mouse Calvaria [Internet]. [cited 2015 Mar 16]. Available from: http://jcb.rupress.org/content/96/1/191.full.pdf
16. Oliveira FA, Matos AA, Santesso MR, Tokuhara CK, Leite AL, Bagnato VS, et al. Low intensity lasers differently induce primary human osteoblast proliferation and differentiation. J Photochem Photobiol B Biol [Internet]. 2016 Oct 1 [cited 2018 Apr 9];163:14–21. Available from: https://www.sciencedirect.com/science/article/pii/S1011134416303128?via%3Dihub
17. Denry I, Kelly JR. State of the art of zirconia for dental applications. Dent Mater. 2008;24(3):299–307.
18. Kohal RJ, Bächle M, Att W, Chaar S, Altmann B, Renz A, et al. Osteoblast and bone tissue response to surface modified zirconia and titanium implant materials. Dent Mater [Internet]. 2013 Jul [cited 2014 Jan 27];29(7):763–76. Available from: http://www.ncbi.nlm.nih.gov/pubmed/23669198
19. Kou W, Akasaka T, Watari F, Sjögren G. An in vitro evaluation of the biological effects of carbon nanotube-coated dental zirconia. ISRN Dent [Internet]. 2013 Jan;2013:296727. Available from: http://www.pubmedcentral.nih.gov/articlerender.fcgi?artid=3762083&tool=pmcentrez&rendertype=abstract
20. de Oliveira PT, Zalzal SF, Beloti MM, Rosa AL, Nanci A. Enhancement of in vitro osteogenesis on titanium by chemically produced nanotopography. J Biomed Mater Res A [Internet]. 2007 Mar 1 [cited 2014 Jan 16];80(3):554–64. Available from: http://www.ncbi.nlm.nih.gov/pubmed/17031821
21. Alves SA, Ribeiro AR, Gemini-Piperni S, Silva RC, Saraiva AM, Leite PE, et al. $TiO_2$ nanotubes enriched with calcium, phosphorous and zinc: promising bio-selective functional surfaces for osseointegrated titanium implants. RSC Adv [Internet]. 2017;7(78):49720–38. Available from: http://xlink.rsc.org/?DOI=C7RA08263K
22. Hanawa T. A comprehensive review of techniques for biofunctionalization of titanium.

J Periodontal Implant Sci [Internet]. 2011 Dec [cited 2014 Feb 25];41(6):263–72. Available from: http://www.pubmedcentral.nih.gov/articlerender.fcgi?artid=3259234&tool=pmcentrez&rendertype=abstract

23. Depprich R, Ommerborn M, Zipprich H, Naujoks C, Handschel J, Wiesmann H-P, et al. Behavior of osteoblastic cells cultured on titanium and structured zirconia surfaces. Head Face Med. 2008;4:29.
24. Yao C, Slamovich EB, Webster TJ. Enhanced osteoblast functions on anodized titanium with nanotube-like structures. J Biomed Mater Res - Part A. 2008;85(1):157–66.
25. Kwun IS, Cho YE, Lomeda RAR, Shin HI, Choi JY, Kang YH, et al. Zinc deficiency suppresses matrix mineralization and retards osteogenesis transiently with catch-up possibly through Runx 2 modulation. Bone [Internet]. 2010;46(3):732–41. Available from: http://dx.doi.org/10.1016/j.bone.2009.11.003
26. Setzer B, Bächle M, Metzger MC, Kohal RJ. The gene-expression and phenotypic response of hFOB 1.19 osteoblasts to surface-modified titanium and zirconia. Biomaterials [Internet]. 2009 Mar [cited 2014 Jan 29];30(6):979–90. Available from: http://www.ncbi.nlm.nih.gov/pubmed/19027946
27. Markwardt J, Friedrichs J, Werner C, Davids A, Weise H, Lesche R, et al. Experimental study on the behavior of primary human osteoblasts on laser-cused pure titanium surfaces. J Biomed Mater Res - Part A. 2014;102(5):1422–30.
28. Ahmad M, Mccarthy M, Gronowicz G. An in vitro model for mineralization of human osteoblast-like cells on implant materials. 1999;20:211–20.
29. Hale L V, Ma YF, Santerre RF. Semi-quantitative fluorescence analysis of calcein binding as a measurement of in vitro mineralization. Calcif Tissue Int [Internet]. 2000 Jul [cited 2014 Jan 13];67(1):80–4. Available from: http://link.springer.com/article/10.1007/s00223001101
30. Bosetti M, Leigheb M, Brooks RA, Boccafoschi F, Cannas MF. Regulation of osteoblast and osteoclast functions by FGF-6. J Cell Physiol. 2010;225(2):466–71.
31. Hempel U, Hefti T, Kalbacova M, Wolf-Brandstetter C, Dieter P, Schlottig F. Response of osteoblast-like SAOS-2 cells to zirconia ceramics with different surface topographies. Clin Oral Implants Res [Internet]. 2010 Mar [cited 2014 Jan 29];21(2):174–81. Available from: http://www.ncbi.nlm.nih.gov/pubmed/19709059
32. Alves SA, Patel SB, Sukotjo C, Mathew MT, Filho PN, Celis JP, et al. Synthesis of calcium-phosphorous doped TiO2nanotubes by anodization and reverse polarization: A promising strategy for an efficient biofunctional implant surface. Appl Surf Sci. 2017;399(December):682–701.

33. Anselme K, Linez P, Bigerelle M, Le Maguer D, Le Maguer A, Hardouin P, et al. The relative influence of the topography and chemistry of TiAl6V4 surfaces on osteoblastic cell behaviour. Biomaterials. 2000;21:1567–77.
34. Titushkin I, Cho M. Modulation of cellular mechanics during osteogenic differentiation of human mesenchymal stem cells. Biophys J [Internet]. 2007 Nov 15 [cited 2013 Dec 16];93(10):3693–702. Available from: http://www.pubmedcentral.nih.gov/articlerender.fcgi?artid=2072058&tool=pmcentrez&rendertype=abstract
35. Meng Y, Qin Y-X, DiMasi E, Ba X, Rafailovich M, Pernodet N. Biomineralization of a self-assembled extracellular matrix for bone tissue engineering. Tissue Eng Part A [Internet]. 2009 Feb;15(2):355–66. Available from: http://www.pubmedcentral.nih.gov/articlerender.fcgi?artid=2782659&tool=pmcentrez&rendertype=abstract
36. Zambuzzi WF, Bruni-Cardoso A, Granjeiro JM, Peppelenbosch MP, De Carvalho HF, Aoyama H, et al. On the road to understanding of the osteoblast adhesion: Cytoskeleton organization is rearranged by distinct signaling pathways. J Cell Biochem. 2009;108(1):134–44.
37. Anderson HC. Matrix vesicles and calcification. Curr Rheumatol Rep. 2003;5(3):222–6.
38. Hale JE, Chin JE, Ishikawa Y, Paradiso PR, Wuthier RE. Correlation between distribution of cytoskeletal proteins and release of alkaline phosphatase-rich vesicles by epiphyseal chondrocytes in primary culture. Cell Motil. 1983;3(5):501–12.
39. Thouverey C, Strzelecka-Kiliszek A, Balcerzak M, Buchet R, Pikula S. Matrix vesicles originate from apical membrane microvilli of mineralizing osteoblast-like saos-2 cells. J Cell Biochem. 2009;106(1):127–38.

**Figure captions:**

**Figure 1:** Representative micrographs of the analyzed biomaterials: cp-Ti (A, D, G), Anod Ti (B, E, H) and zirconia (C, F, I). 3D surface reconstructions by confocal microscopy (A, B, C) were used for roughness measurements using Leica MAP software. The same fields are seen in the topographic images (D, E, F). In F the scalebar unit is nm. SEM (D, E, F) imaging confirm the morphological characteristics. Scale bar 20 µm.

**Figure 2:** Average area roughness (Sa) analysis data for cp-Ti, anodized Ti and zirconia.

**Figure 3:** Confocal images showing the osteoblast morphological changes and mineralization nodules over time. Osteoblasts over cp-Ti, anodized titanium and zirconia cultured for 7, 14 and 21 days. Calcein labeling (green fluorescence) reveals mineralization nodules. Actin cytoskeleton is detected by Rhodamine phalloidin in red. Blue fluorescence (DAPI DNA stain) indicates cell nuclei. Scalebar: 50 µm.

**Figure 4:** Volume measurement results for mineralization. Logarithmic scale was used for the y axis.

**Figure 5:** Volume measurement results for actin cytoskeleton.

**Figure 6:** Correlation data between mineralization and actin cytoskeleton volumes on all materials, for all culture times. A weak negative linear relationship with Pearson´s coefficient r=-0.21 was obtained.

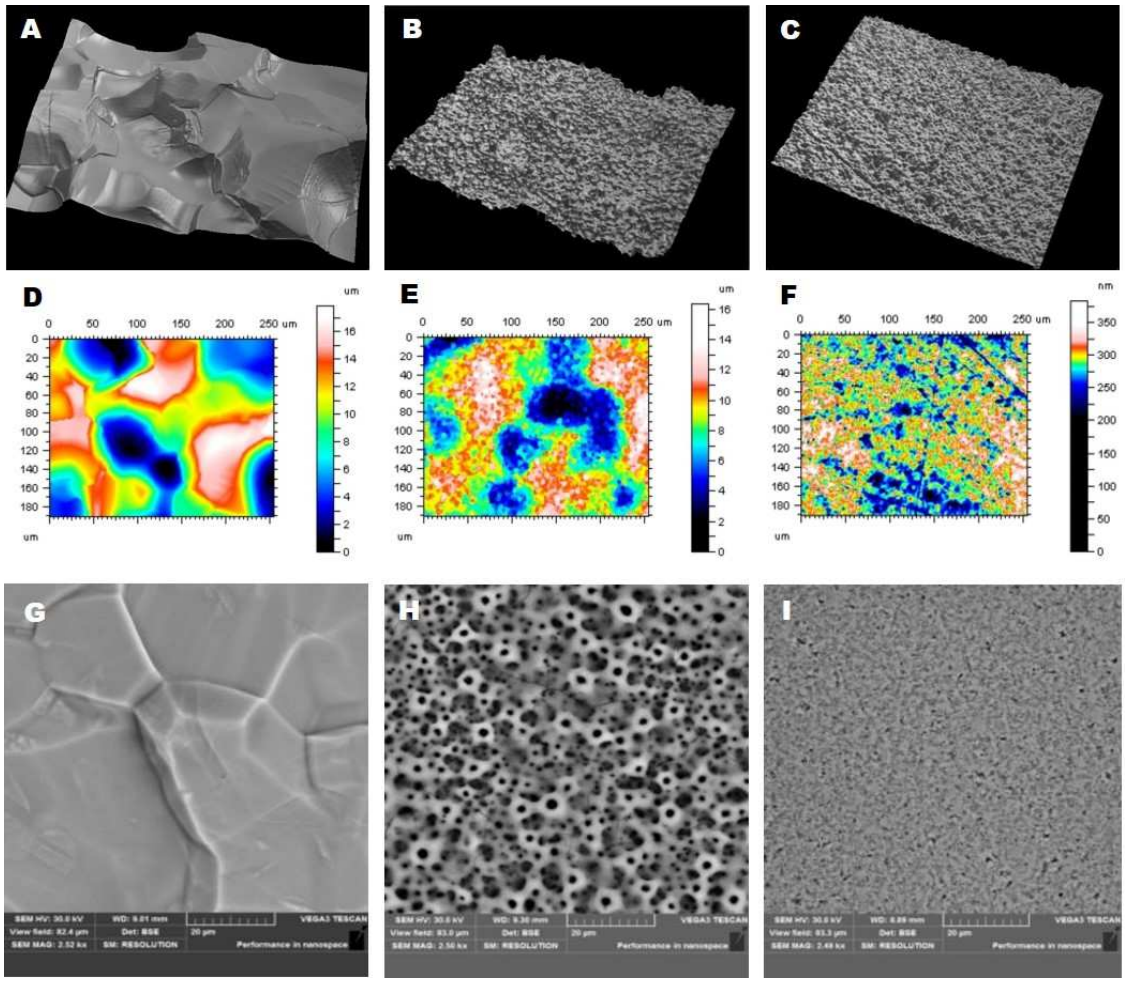


Figure 1

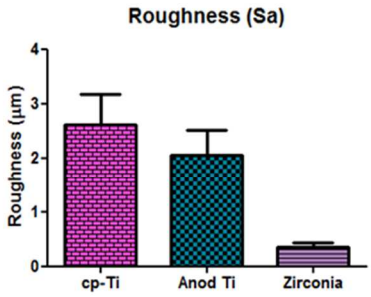


Figure 2

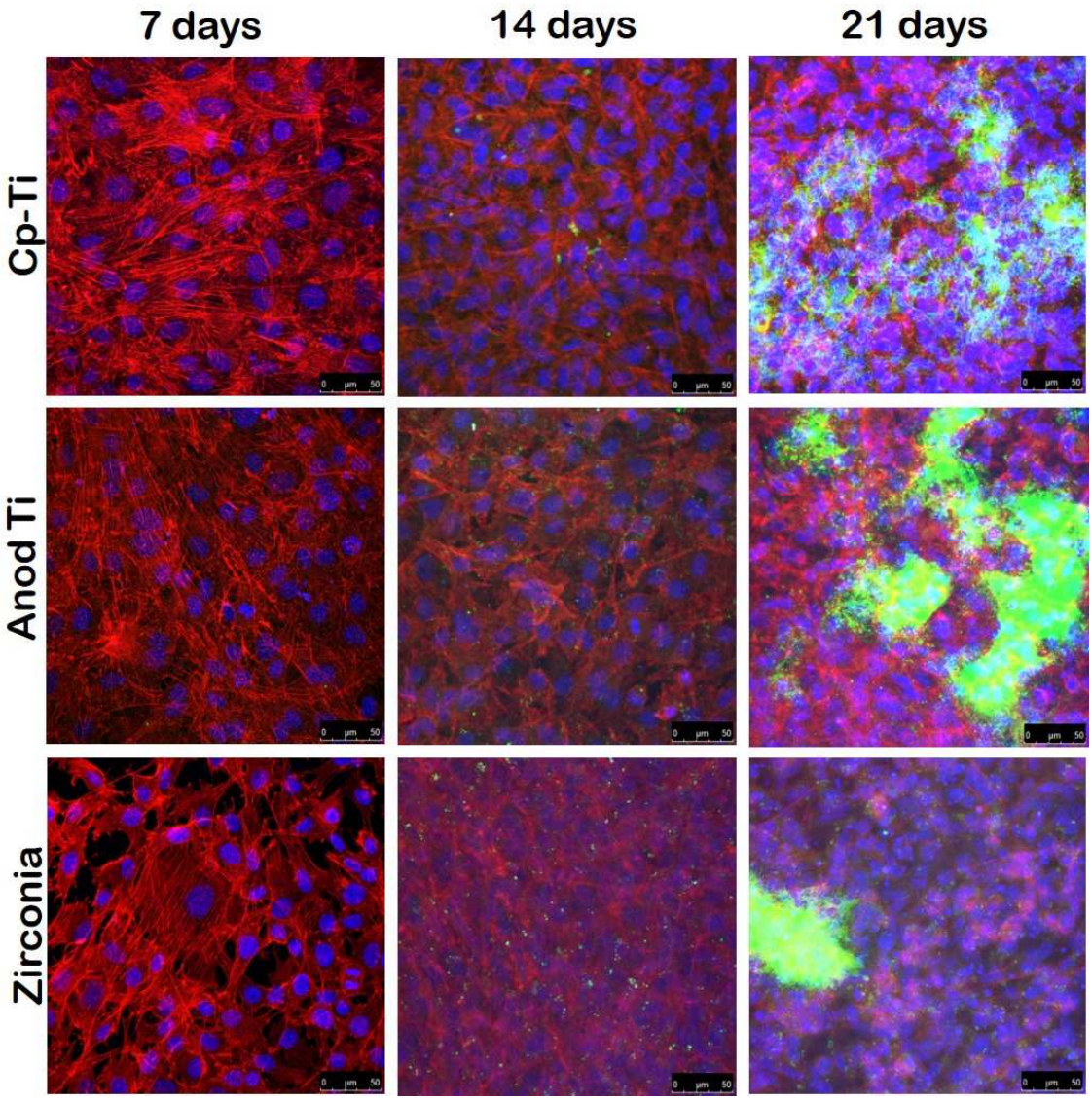


Figure 3

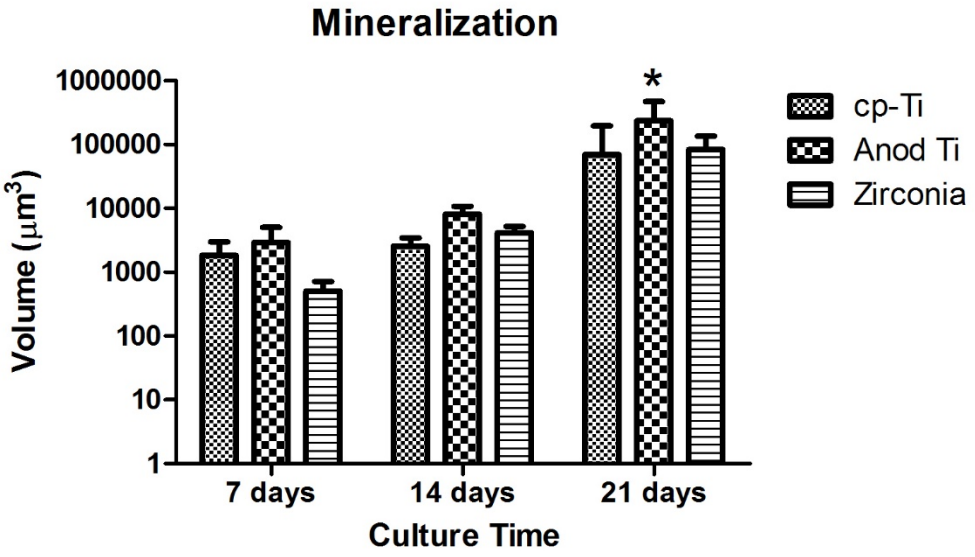


Figure 4

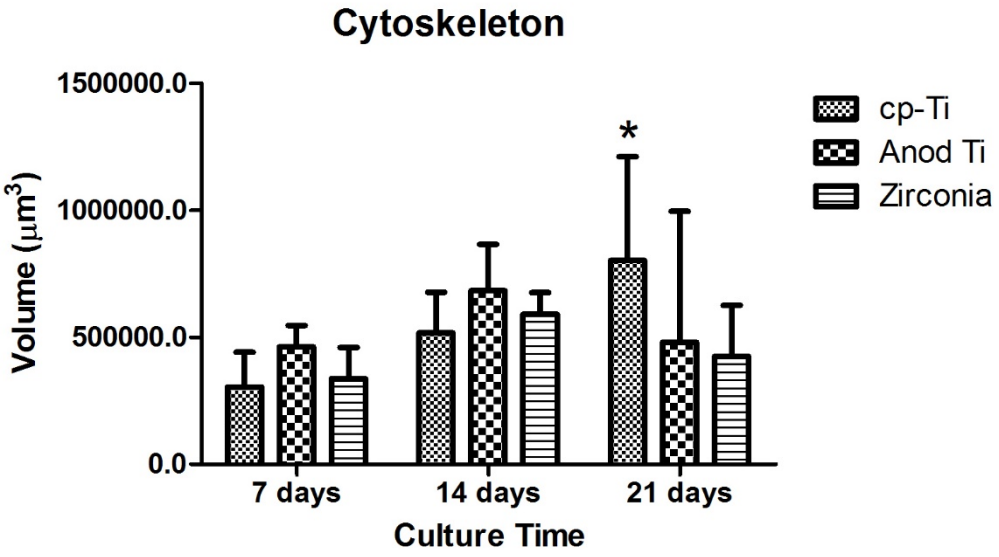


Figure 5

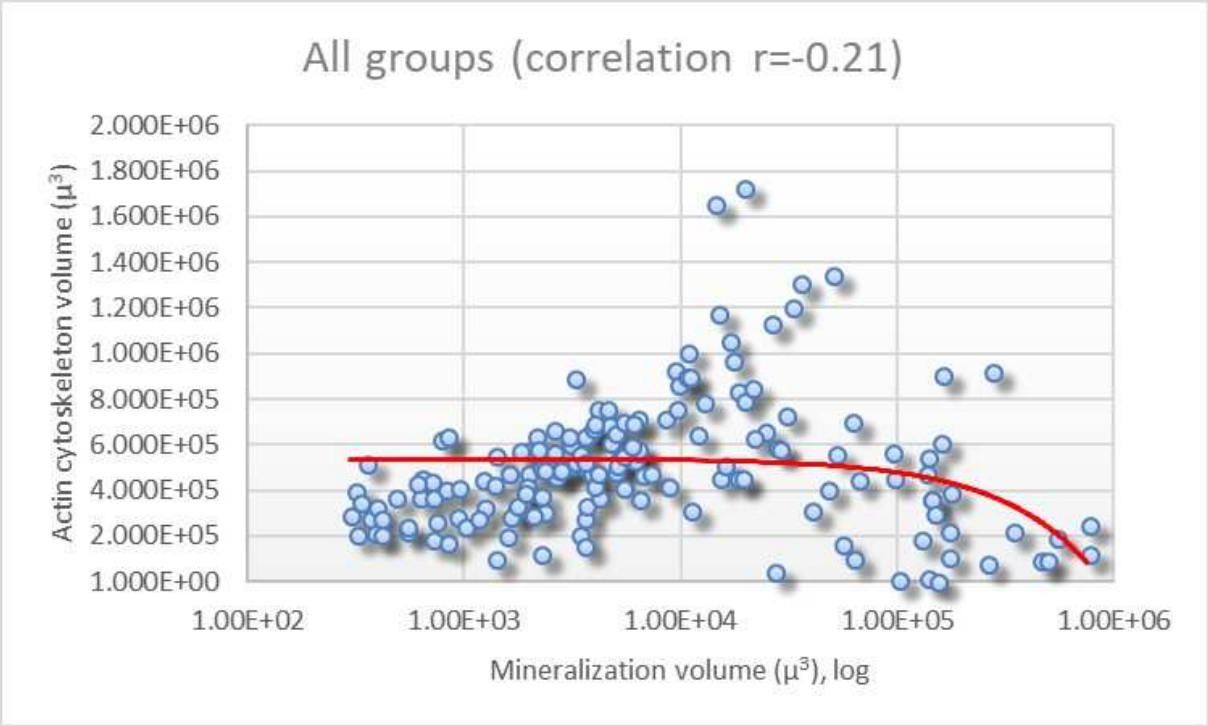
All groups (correlation r=-0.21)
Actin cytoskeleton volume (µ³)
2.000E+06
1.800E+06
1.600E+06
1.400E+06
1.200E+06
1.000E+06
8.000E+05
6.000E+05
4.000E+05
2.000E+05
1.000E+00
1.00E+02
1.00E+03
1.00E+04
1.00E+05
1.00E+06
Mineralization volume (µ³), log

Figure 6

## 2.2 ARTICLE 2

# Longitudinal comparison of the ECM proteins from osteoblasts cultivated on different biomaterials

Graeff MSZ[1], Tokuhara CK[2], Sanches MLR[2], Oliveira RC[1,2,3]

*1 Centro Integrado de Pesquisas CIP 1 Faculdade de Odontologia de Bauru- FOB/USP*
*2 Departamento de Ciências Biológicas, Faculdade de Odontologia de Bauru- FOB/USP*
*3Braço Brasileiro do Instituto de Biomateriais, Tribocorrosão e Nanomedicina (IBTN/Br)*
*email: mszgraef@usp.br*

**Abstract**

Dental implant failures cause patient discomfort and often clinical bone loss. It is therefore important to assure good osseointegration capability and avoid corrosion. Although being the current gold standard for metal implants, titanium is subject to long- term corrosion. The incorporation of Mg, Ca and P in the structure of titanium oxide films produced by anodization has improved tribocorrosion resistance. Yttria stabilized zirconia (Y-TZP) has become a material of choice when considering aesthetic results. The extracellular matrix (ECM) has important roles in regulating the cellular response to surfaces. However, very little is still known about the proteomics of bone matrix mineralization. Our objective was a longitudinal comparison of the ECM proteins from osteoblasts cultivated on cp-Ti grade 2, anodized titanium and Y-TZP by mass spectrometry. MC3T3 cells were plated at a density of $10^5$ cells on 12 samples of each group and cultivated for 7, 14 and 21 days, with osteogenic media. Afterwards, the specimens were washed, decellularized and the ECM was collected in buffer solution. Conclusion: The original method used to limit the number of analyzed proteins was efficient. The majority of the typical ECM proteins are expressed and regulated equally on the three biomaterials tested. Involved in metabolic processes, Alpha-1_4 glucan phosphorylase and Glycogen phosphorylase brain form were differentially expressed on zirconia and anodized titanium , perhaps due to surface characteristics. Proteins related to bone development like Transforming growth factor beta-3 and Fibroblast growth factor 8 were found exclusively on cp-Ti on the 21$^{st}$ day. Our results reveal new insights regarding osseointegration and how material surfaces affect this process.

**Introduction**

Concerning dental implants, the most commonly used biomaterial is titanium. It has been reported that corrosion and tribocorrosion processes affect titanium implants, sometimes leading to implant loss or gingival darkening. One appointed solution is the replacement of titanium for an inert material like zirconia[1], whose color mimic that of natural enamel[2]. Surface modifications can improve tribocorrosion performance by changing composition, morphology or structure, while keeping unaltered the substrate

mechanical properties. Oxidative anodization has been widely used on this purpose, overcoming corrosion issues[3].

Cellular responses to material surfaces are determinant for a successful implant performance. After adhering, proliferating and spreading over the implant surfaces, it is mandatory for the osteoblasts to be able to generate bone around the implant, a process called osseointegration, which guarantees the long-term stability of the implant[4].

A key factor in cell-biomaterial interactions is the extracellular matrix (ECM). Besides directing important events such as cell proliferation, survival, differentiation, and migration, it provides structural support for the cells within a tissue. Composed of water, collagens, glycoproteins and proteoglycans, the ECM is a complex structure that is constantly being remodeled[5].

Bone formation is a not fully understood process, which involves mineralization of the extracellular matrix by the deposition of hydroxyapatite, rich in calcium and other minerals. Grzesiak et al. (2017) concluded that this process is connected with cell death and mineralization nodules derive from calcium rich cellular remnants[6].

The field of proteomics has contributed to the understanding of many cellular processes. Still, very little is known about the ECM proteomics during mineralization. The protein profiles of the ECM and matrix vesicles (MVs) of mineralizing osteoblasts were described for the first time in the work of Xiao et al (2007)[7]. The cells were cultivated on conventional culture plates, and the cellular content was separated from the ECM proteins by gel electrophoresis. However, this work had no relation to biomaterials interaction.

Comparison of the whole proteomic profiles of human osteoblasts grown over two biomaterials was conducted by Jinling Xu (2008)[8], but only for an initial phase (4 days of incubation). A description of the protein content of the isolated ECM was presented by Rashid et al (2012)[9]. using an *in vitro* model of fibrotic liver tissue, where the samples were decellularized. This interesting approach directs the proteomic analysis to a focused dataset.

In this work, we aimed to compare the proteome of decellularized ECM generated by murine preosteoblasts grown over three different biomaterials after 7, 14 and 21 days of culture.

## Material and Methods

*Sample preparation*

Commercially pure titanium grade 2 (cp-Ti) was used as control group and the bulk material for the anodization process, as described in the work of Ribeiro et al (2015)[10]. The specimens were square shaped, 10 x 10 x 2 mm in size. To remove the native oxide layer, all 72 metal samples were etched individually in a solution containing nitric acid ($HNO_3$), fluoridric acid (HF) and distilled water in equal proportions (1:1:1) for 15 seconds. This process was followed by a bath in ethylic alcohol with ultrasound for 15 min and drying in drying oven. Afterwards, the specimens were separated in two groups of 36 samples each, namely, cp-Ti and Anod Ti.

The solution used for the anodic treatment consisted of 0.02M β-glycerophosphate disodium salt pentahydrate, 0.35M calcium acetate monohydrate and 0.1 M of Magnesium acetate monohydrate, all dissolved in ultra-pure distilled water. Using a platinum rod as the counter electrode, at a constant

voltage of 300 V and under magnetic agitation, each specimen was anodized separately for 1 min, and then taken to a drying oven for 4 hours.

The yttria stabilized zirconia block (Y-TZP) was acquired from Ivoclar Vivadent (ref. IPS e.max ZirCAD) and cut into 12.5 x 12.5 x 3.0 mm square pieces. Silicon carbide sandpaper (600 grit) was used to manually sand the samples. An inFire HTC Speed (Sirona) oven was used for sintering, as indicated by the supplier. The final size was 10 x 10 x 2 mm. Afterwards, the zirconia samples were washed with detergent under running water, cleaned by sonication in deionized water for 10 min and dried with hot air blow.

Atomic force microscopy (AFM) was used to check the surface topography and texture of the biomaterials. For each group, three samples were taken to a Bruker Dimension Icon microscope where six fields were imaged on each sample. Finally, all samples were autoclaved for 15 min at 120°C and dried overnight in a drying oven, before being used for cell culture.

*Cell culture and ECM collection.*

Divided in three groups (7, 14 or 21 days) of twelve samples each, a total of thirty-six specimens of each material were used for cell culture. Murine preosteoblastic MC3T3 cells (ATCC® CRL-2593™)[11], passage number 13, were plated at a density of $10^5$ cells on each specimen, and cultivated for 7, 14 and 21 days, in osteogenic media. Basically, α-MEM media supplemented with 10% BFS, 50 µg.mL-1 acid ascorbic and 10 mM β-glicerophosphate (Sigma®) was used, and half of the media was changed every third day.

After the established culture time, the specimens were washed twice with lukewarm PBS, and decellularized with a solution containing 20mM $NH_4OH$ and 0.5% (v/v) Triton X-100 in PBS, for 1 minute at 37°C[9]. Afterwards, the samples were washed twice with PBS to remove cell debris and kept over ice during ECM collection. For each group, a separate well of a 12-well plate was used. The plate was kept over ice and 1ml of lysis buffer (7 M urea, 2 M thiourea, 40 mM DTT, all diluted in AMBIC solution) was added to the well. Each sample was scraped with a cell scraper (Corning) and the ECM lysates from the 12 samples of the same group were pooled and collected into 1.5-mL mini-centrifuge tubes (Axygen, Union City, CA). Afterwards, 600µL of lysis buffer was added to the same well and the samples were scraped again. Protease inhibitor cocktail (Sigma, USA) at 1% (v/v) was added to each tube and stored at -80°C.

*Proteomic Analysis*

After thawing on ice for 3 hours, pellets were dissolved by sonification at 60% amplitude and maximum temperature of 18 °C (Bransons Ultrasonics, Danbury, CT) until no aggregates were visible. Samples were centrifuged at 5000 rpm for 5 min at 4 °C and the supernatant was collected. The protein concentration of the ECM lysates was determined with the Bradford protein dye (BioRad Laboratories, Hercules, CA).

The volumes containing 50 µg protein were calculated for each group and separated. Then 10 µL 50 mM AMBIC and 25 µL of 0.2% Rapigest (WATERS cat#186001861) were added to each sample, agitated in vortex and incubated for 30 min at 37 °C. Reduction was performed by the addition of 2.5 µL 100 mM DT (BIORAD, cat# 161–0611), agitation in vortex and incubation for 40 min at 37 °C.

Samples were alkylated with 2.5 µL 300 mM IAA (GE, cat# RPN 6302 V) at room temperature for 30 min in the dark. Digestion was performed by adding 100 ng trypsin (PROMEGA, cat #V5280) at 37 °C overnight.

From this point on, the samples preparation, peptides identification by LC-MS/MS and bioinformatics analyses followed the protocol described by Dionizio (2017)[12]. Bioinformatics analysis was done to compare both Anod Ti and zirconia ECM proteins to that of cp-Ti at each time point. In total, six comparisons were made, where only the uniquely or differentially expressed proteins were considered. Networks of molecular interactions between the identified proteins were built using the software CYTOSCAPE 3.6.1 (JAVA), as well as clusterMaker application. The gene ontology application ClueGo was used to categorize the proteins for their annotation relative to biological processes and molecular functions.

## Results

*AFM imaging*

The biomaterial surfaces were imaged by AFM (Figure 1). Inside each group, the samples were identical, presenting homogeneous surfaces. A granular texture was observed on the cp-Ti surface. The anodization process induced a porous characteristic over the granular topography provided by the titanium bulk. On the other hand, zirconia surface is flat and smooth. A broader characterization of the same biomaterials was done by our group in other study.

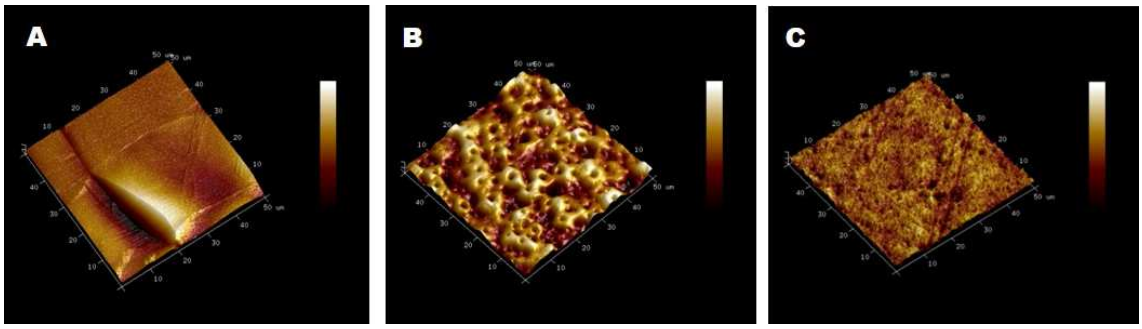


**Figure 1:** Representative images of the biomaterials surfaces. Cp-Ti (A), Anod Ti (B) and zirconia (C). Field dimensions: 50 µm x 50 µm. Maximum height: 10 µm (A and B), 1 µm (C).

*Proteomic Analysis*

A total of 24 proteins were identified, being uniquely or differentially expressed among groups. Proteins access numbers, as well as their subcellular location, were checked at UNIPROT. . The small number of identified proteins attests for the efficacy of the decellularization process adopted.
After 7 days of culture, three proteins were uniquely expressed on cp-Ti when compared to Anod Ti and zirconia, while only one was found uniquely on Anod Ti and five proteins were uniquely identified on zirconia (Tables 1 and 2). On the 14$^{th}$ day, four and two proteins were uniquely found on Anod Ti and zirconia, respectively (Tables 3 and 4). Six proteins were found uniquely expressed on cp-Ti when

compared to Anod Ti on the 21st day of culture. The same six proteins were also found uniquely on cp-Ti when compared to Zirconia on the same day (Tables 5 and 6).

In all comparisons, only two proteins with change in expression were detected (Table S7). The Alpha-1,4 glucan phosphorylase (E9PUM3) was found to be down-regulated on zirconia on the 7th day, while at the same time, Glycogen phosphorylase brain form (Q8CI94) was up-regulated on Anod Ti. After 14 days of culture, Glycogen phosphorylase brain form was down-regulated on zirconia.

**Table 1.** Uniquely expressed proteins identified in the comparison Anod Ti vs cp-Ti at 7th day**.**

| Access Number | Protein Name | *PLGS Score* | Unique |
|---|---|---|---|
| Q9DAA4 | Probable inactive serine protease 37 | 48.47 | cp-Ti at 7th day |
| Q61858 | G patch domain and ankyrin repeat-containing protein 1 | 86.64 | cp-Ti at 7th day |
| Q6PES3 | Bat4 protein | 74.71 | cp-Ti at 7th day |
| A2AL36 | Centriolin | 119.91 | Anod Ti at 7th day |

**Table 2.** Uniquely expressed proteins identified in the comparison zirconia vs cp-Ti at 7th day.

| Access Number | Protein Name | *PLGS Score* | Unique |
|---|---|---|---|
| Q9DAA4 | Probable inactive serine protease 37 | 48.47 | cp-Ti at 7th day |
| Q61858 | G patch domain and ankyrin repeat-containing protein 1 | 86.64 | cp-Ti at 7th day |
| Q6PES3 | Bat4 protein | 74.71 | cp-Ti at 7th day |
| Q6PAJ1 | Breakpoint cluster region protein | 52.50 | zirconia at 7th day |
| Q8VI56 | Low-density lipoprotein receptor-related protein 4 | 32.93 | zirconia at 7th day |
| Q9DBA8 | Probable imidazolonepropionase | 41.10 | zirconia at 7th day |
| Q9R1S0 | B9 domain-containing protein 1 | 103.16 | zirconia at 7th day |
| Q3UKK2 | Carcinoembryonic antigen-related cell adhesion molecule 5 | 43.96 | zirconia at 7th day |

**Table 3.** Uniquely expressed proteins identified in the comparison Anod Ti vs cp-Ti at 14th day.

| Access Number | Protein Name | *PLGS Score* | Unique |
|---|---|---|---|
| A2AF47 | Dedicator of cytokinesis protein 11 | 54.48 | Anod Ti at 14th day |
| Q9JL35 | High mobility group nucleosome-binding domain-containing protein 5 | 62.14 | Anod Ti at 14th day |
| A2AG50 | MAP7 domain-containing protein 2 | 54.83 | Anod Ti at 14th day |
| P61600 | N-alpha-acetyltransferase 20 | 133.63 | Anod Ti at 14th day |

**Table 4.** Uniquely expressed proteins identified in the comparison zirconia vs cp-Ti at 14th day

| Access Number | Protein Name | *PLGS Score* | Unique |
|---|---|---|---|
| F7CEK4 | Protein unc-13 homolog B (Fragment) | 109.80 | zirconia at 14th day |
| Q8CII0 | Zinc finger and BTB domain-containing protein 8B | 49.66 | zirconia at 14th day |

**Table 5.** Uniquely expressed proteins identified in the comparison Anod Ti vs cp-Ti at 21st day.

| Access Number | Protein Name | *PLGS Score* | Unique |
|---|---|---|---|
| P47936 | Cannabinoid receptor 2 | 154.51 | cp-Ti at 21st day |
| P37237 | Fibroblast growth factor 8 | 59.20 | cp-Ti at 21st day |
| P17125 | Transforming growth factor beta-3 | 61.96 | cp-Ti at 21st day |
| Q3TA38 | Transmembrane protein 120B | 83.79 | cp-Ti at 21st day |
| P20152 | Vimentin | 174.15 | cp-Ti at 21st day |
| E9QAH2 | Zinc finger protein 605 | 76.08 | cp-Ti at 21st day |

**Table 6.** Uniquely expressed proteins identified in the comparison zirconia vs cp-Ti at 21st day

| Access Number | Protein Name | *PLGS Score* | Unique |
|---|---|---|---|
| P47936 | Cannabinoid receptor 2 | 154.51 | cp-Ti at 21st day |
| P37237 | Fibroblast growth factor 8 | 59.20 | cp-Ti at 21st day |
| P17125 | Transforming growth factor beta-3 | 61.96 | cp-Ti at 21st day |
| Q3TA38 | Transmembrane protein 120B | 83.79 | cp-Ti at 21st day |
| P20152 | Vimentin | 174.15 | cp-Ti at 21st day |
| E9QAH2 | Zinc finger protein 605 | 76.08 | cp-Ti at 21st day |

**Table 7.** Proteins that showed significant changes (0.05 < p-value < 0.95) in expression in all 6 comparisons done.

| Access Number | Protein Name | *PLGS Score* | Probability | Ratio | Comparison |
|---|---|---|---|---|---|
| Q8CI94 | Glycogen phosphorylase_ brain form | 236,59 | p=0,96 ↑ | 1.06 | Anod Ti X cp-Ti at 7th day |
| E9PUM3 | Alpha-1_4 glucan phosphorylase | 1177.82 | p=0.07 ↓ | 0.97 | zirconia X cp-Ti at 7th day |
| Q8CI94 | Glycogen phosphorylase_ brain form | 227.65 | p=0.03 ↓ | 0.90 | zirconia X cp-Ti at 14th day |

Figure 2 shows the subnetworks created by clusterMaker for the 24 proteins identified in this work. Among these, only 11 proteins had known interactions, according to the datasets consulted.

A structural protein that acts as intermediate filament, Vimentin (P20152), was found only on cp-Ti after 21 days of culture. It was indirectly associated with G patch domain and ankyrin repeat-containing protein 1 (Q61858, found uniquely on cp-Ti on the 7th day) via Nucleophosmin (Q61937), which is a chaperone protein, not identified in this work.

Vimentin was also associated with Probable imidazolonepropionase (Q9DBA8, identified solely on zirconia after 7 days of culture) via 6-Phosphogluconolactonase (Q9CQ60), not identified in this work. These associations are described in the literature in colocalization studies.

Glycogen phosphorylase brain form, identified as up-regulated on Anod-Ti at day 7 and down-regulated on zirconia after 14 days, is associated with 14–3-3 protein epsilon (P62259), not identified in this work. P62259 also interacts with High mobility group nucleosome-binding domain-containing protein 5 (Q9JL35), found uniquely on Anod Ti on the 14th day. These associations were also described by imaging colocalization methods.

Breakpoint cluster region protein (Q6PAJ1), B9 domain-containing protein 1(Q9R150), Low-density lipoprotein receptor-related protein 4 (Q8VI56), and Dedicator of cytokinesis protein 11 (A2AF47) only have associations with proteins not identified in this work, which are shown as gray colored blocks on the networks provided.

Breakpoint cluster region protein is a GTPase-activating protein for RAC1 and CDC42. It was identified as unique to zirconia at the 7$^{th}$ day and was associated with Vascular SH2 domain-containing protein (A2AM67, unreviewed), Reverse transcriptase (Q8J7W5, unreviewed) and Cell cycle progression protein 1 (Q640L3).

Low-density lipoprotein receptor-related protein 4 (Q8VI56, lrp-4) mediates the endocytosis of cholesterol-rich LDL. Seven proteins are described in the same subnetwork with lrp-4: LRP chaperone MESD (Q9ERE7), Muscle, skeletal receptor tyrosine-protein kinase (Q61006), C-Jun-amino-terminal kinase-interacting protein 1 (Q9WVI9-1, involved in vesicle-mediated transport), Protein interacting with C kinase 1 (Q80VC8), Ran-binding protein 9 (P69566), Sortilin-related receptor (088307), and Agrin (A2ASQ1).

Dedicator of cytokinesis protein 11 (A2AF47), also involved in the molecular function of Rho GTPase binding, interacts with DNA polymerase beta (P06766). Centriolin (A2AL36) and Fibroblast growth factor 8 (P37237) had no known associations on the databases consulted.

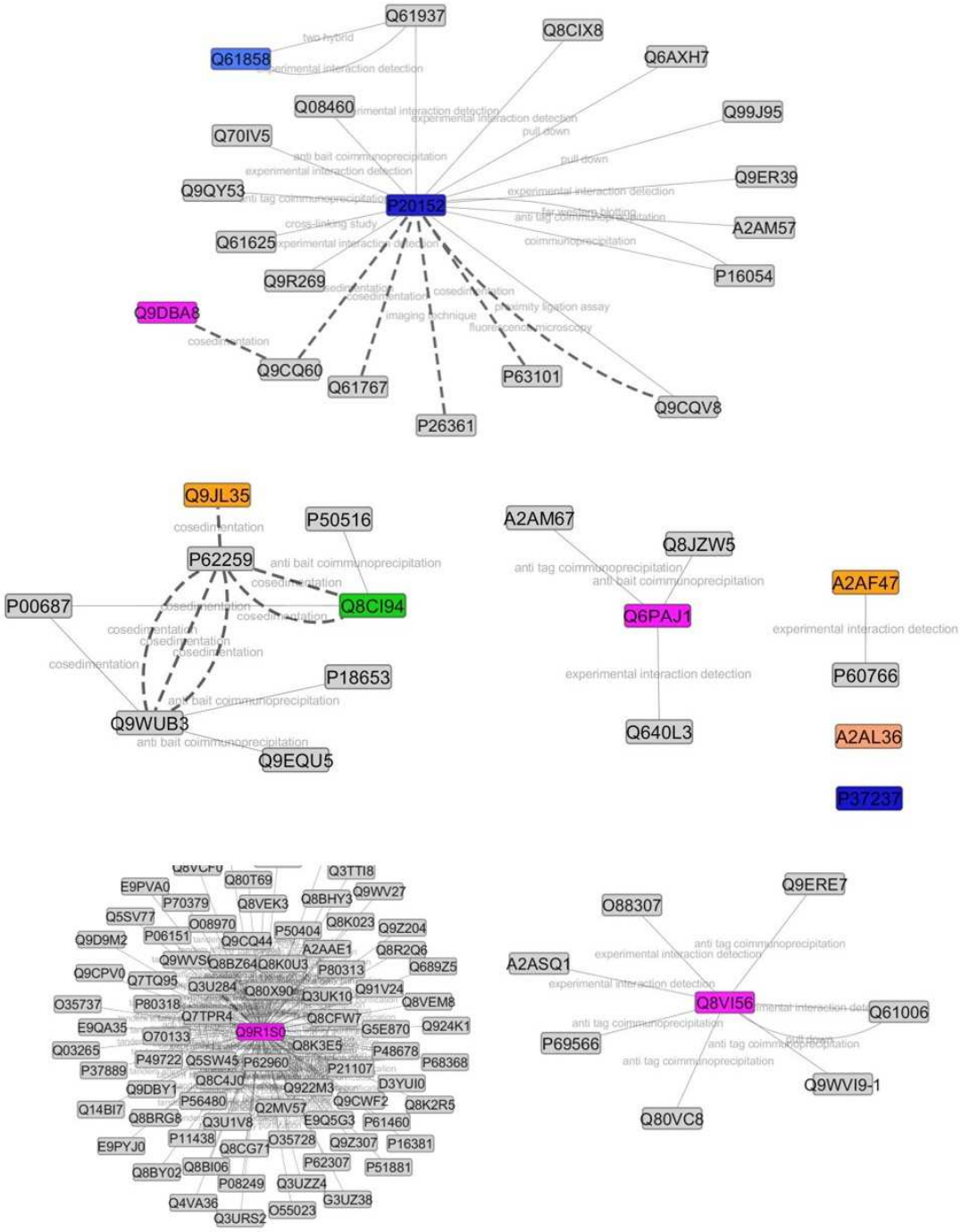


**Figure 2:** ClusterMaker subnetworks demonstrates the interaction between proteins with differential or unique expression in all comparisons. The boxes were color-coded for groups. Light blue represents proteins exclusively identified on Cp-Ti after 7 days of culture and dark blue proteins on cp-Ti on the 21st day. Proteins uniquely found on Anod Ti on the 7th day were colored in light orange while dark orange represents those found on Anod Ti after 14 days of culture. Magenta stands for proteins solely found on Zirconia after 7 days. Differentially expressed proteins were colored green. Gray boxes stand for proteins related to those mentioned above but not identified in this study. Dashed lines represent studies where the related proteins were found colocalized, while continuous lines represent other forms of association.

Figure 3 depicts the significant biological processes into which the proteins with differential or unique expression in all comparisons were categorized, according to ClueGo® 2.5.1 (considering a kappa score ≥ 0.4). The categories with the highest percentage of associated genes were glycogen catabolic process (50%) and positive regulation of collagen biosynthetic process (50%).

To understand the biological relevancy of the identified proteins, a functional analysis was made. Figure 4 shows the molecular function distribution obtained with ClueGO®. The highest number of associated genes were related to Rho GTPase binding (33%), glycogen phosphorylase activity (22%), imidazolonepropionase activity (11%), peptide alpha-N-acetyltransferase activity (11%), nucleosomal DNA binding (11%) and hedgehog receptor activity (11%).

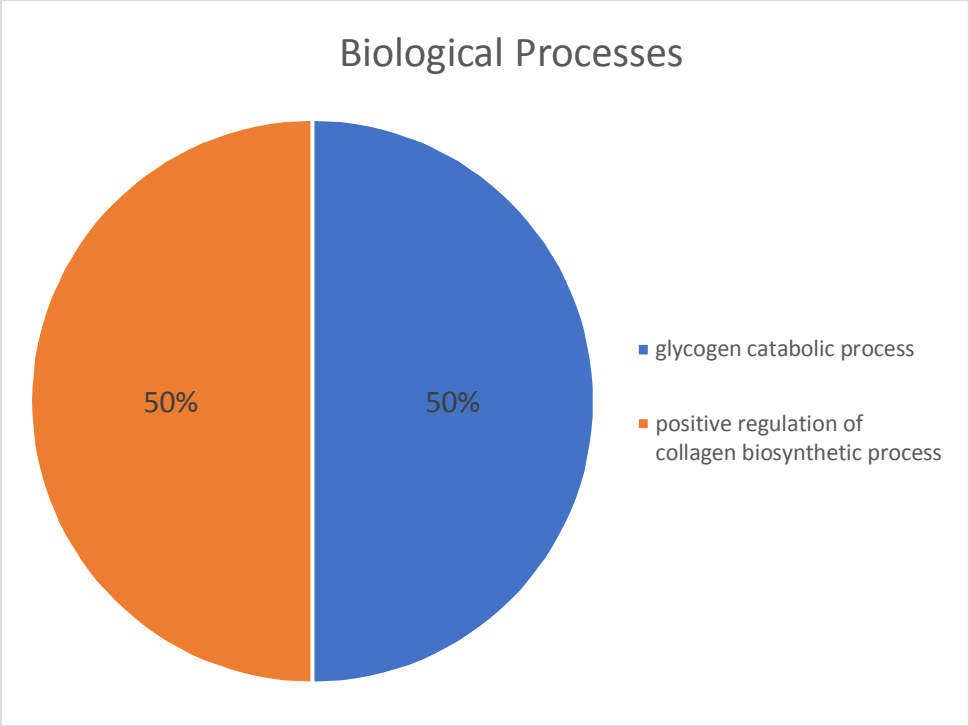


**Figure 3:** Biological processes associated with the proteins identified as unique or differentially expressed on all the groups studied, based on GO annotation Biological Process. The gene ontology was evaluated according to ClueGo® 2.5.1 pluggins of Cytoscape® software 3.6.1.

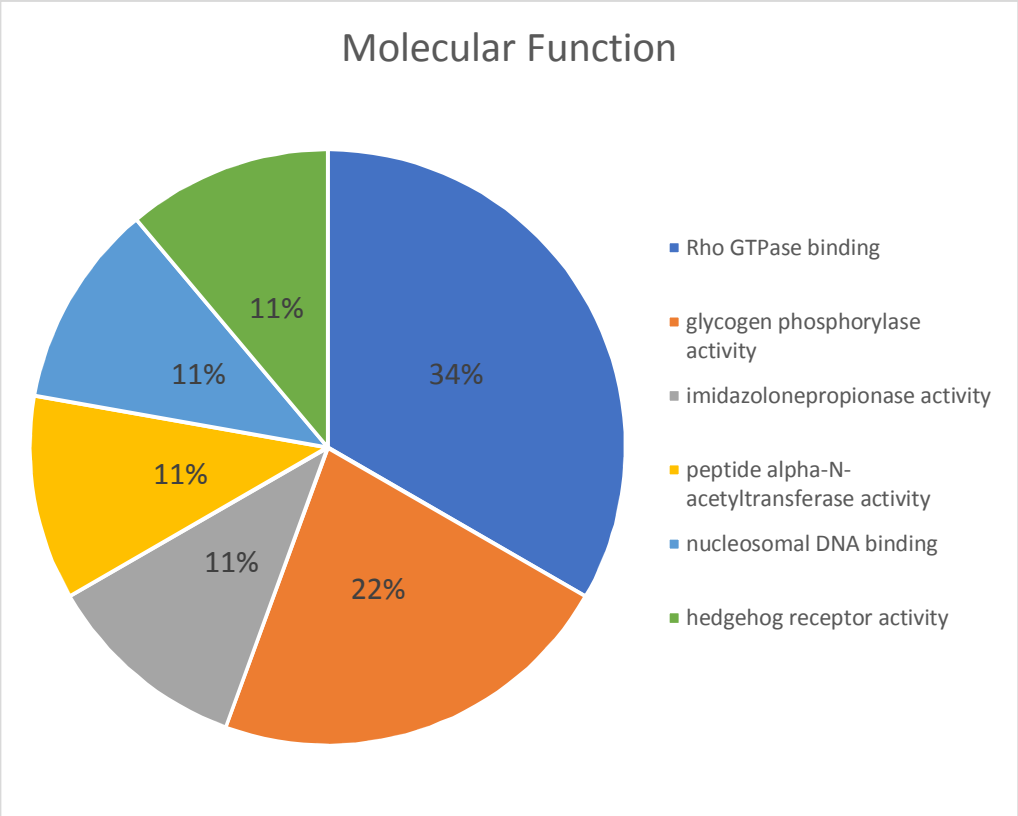


**Figure 4:** Functional distribution of the proteins identified as unique or differentially expressed on all the groups studied, based on GO annotation Molecular Function. The gene ontology was evaluated according to ClueGo® 2.5.1 pluggins of Cytoscape® software 3.6.1.

## Discussion

Much of the pivotal role ECM proteins play in osseointegration remains unclear. As previously mentioned, ECM components participate in cellular signaling, besides providing structural support. Many research efforts are focused on ECM description, trying to elucidate its complex composition and dynamical behavior[5]. We employed a proteomic approach to evaluate differences in ECM protein expression from osteoblasts cultivated on three different implant surfaces, and how it changes over time.

Our results revealed that the great majority of the typical ECM proteins are expressed and regulated equally on the three biomaterials tested, albeit distinct chemical compositions and surface roughness. Some proteins identified were uniquely found on a biomaterial at certain time points, whereas only two proteins were up or down-regulated.

Some proteins identified in the collected ECMs are classified as membrane receptors and growth factors or associated to molecular signaling pathways, normally found in the extracellular region. B9 domain-containing protein 1 (Q9R1S0) is required for sonic hedgehog/Shh signaling and was uniquely found on zirconia on the 7$^{th}$ day. The importance of the Shh signaling system in osteoblast morphological changes when cultured in basement membrane matrix (Matrigel™) was evaluated by Marumoto et al (2017)[13]. When Shh was inhibited, a proliferative response was obtained, instead of the morphological changes observed when sonic hedgehog signaling is active. The role of the Hedgehog-Gli1 pathway in the response of osteoblasts to different titanium topographies was evaluated by Lin (2017)[14], and on the nanostructured surface studied, the mRNA expression of Sonic hedgehog (Shh) was higher when

compared to that on the smooth and microstructured surfaces. In our work, the zirconia surface presents irregularities in the nanoscale, which may have caused a similar effect.

Breakpoint cluster region protein was unique to zirconia at 7th day. Being a GTPase-activating protein for the GTPases of the Rho family, it is involved in the regulation of Rho protein signal transduction, negative regulation of cell migration, regulation of cell cycle, actin cytoskeleton organization and intracellular protein transmembrane transport, among other functions. In our work, this protein was found associated with Cell cycle progression protein 1 (Q640L3). The latter is a membrane protein involved in positive regulation of cell cycle and cell proliferation, acting as an assembly platform for Rho protein signaling complexes.

Low-density lipoprotein receptor-related protein 4 (Q8VI56, Lrp4) was uniquely identified on zirconia at the 7th day. In this work, it was associated with Agrin, known to induce an increase in cytoplasmic calcium ions, specifically modulating calcium ion homeostasis in neurons. Xiong et al (2015)[15] identified Lrp4 as a critical player in bone mass homeostasis, acting as a receptor of sclerostin to inhibit Wnt/β-catenin signaling and bone formation.

The work of Sophocleous (2017)[16] indicates that Cannabinoid receptor 2 (P47936, Cnr2) plays a role in regulating bone mass and bone cell activity. Combined deficiency of the Cnr1 and Cnr2 receptors in female mice protects against age-related bone loss due to a reduction in osteoclast number when compared with wild-type. Our results show Cnr2 uniquely expressed on cp-Ti after 21 days of culture, during the mineralization phase.

Identified only on cp-Ti at the 21st day, transforming growth factor beta-3 (Q91YU7, TGF-β3) is typically found in the extracellular region. Among other functions, it participates in the positive regulation of bone mineralization and positive regulation of collagen biosynthetic process. In a very elegant study of Wang et al (2012)[17], the relations between collagen XXIV, TGF-β e Smad were demonstrated in MC3T3 cells. Interestingly, a recent work by Deng (2017)[18] reports that TGFβ3 could recruit MSCs to initiate bone regeneration.

Another grow factor identified in this work, typical of the extracellular region, Fibroblast growth factor 8 (P37237) was found exclusively expressed on cp-Ti at the 21st day. It plays an important role in the regulation of embryonic development, cell proliferation, cell differentiation and cell migration. Valta et al (2006)[19] showed that besides inducing osteoblast differentiation, FGF-8 stimulates the proliferation of cultured mouse bone marrow cells efficiently and induced their early stage differentiation. The stimulatory effects of FGF-8 on osteoblast proliferation in primary osteoblast cultures was also proved in a study by Lin et al (2009)[20], while in long-term cultures of osteoblasts, nodule formation was inhibited.

Cytoskeleton associated proteins like centriolin (A2AL36, unique to Anod Ti at the 7th day), MAP7 domain-containing protein 2 (A2AG50, unique to Anod Ti at the 14th day), and vimentin were also identified. Vimentins are class-III intermediate filaments, localized in the extracellular matrix or as part of the cytoskeleton. According to Gene Ontology, it is involved in the positive regulation of collagen biosynthetic process and SMAD protein signal transduction. In this work vimentin was identified as exclusive for the cp-Ti group after 21 days of culture, being indirectly associated with G patch domain and ankyrin repeat-containing protein 1 (Q61858, found on cp-Ti on the 7th day). Another association was with Probable imidazolonepropionase (Q9DBA8, identified on zirconia after 7 days of culture) via 6-Phosphogluconolactonase (Q9CQ60).

One specific association between osteoblasts and vimentin was described by Lian et al. (2009)[21], where vimentin inhibited differentiation in immature osteoblasts by interacting with Activating transcription factor 4 (ATF4). Later, in 2012, Lian et al[22] described this process in detail, stating that TGF-β stimulates vimentin production, leading to suppression of ATF4-dependent osteocalcin (Ocn) transcription and osteoblast differentiation. Schmidt et al (2015)[23] demonstrated that alkaline phosphatase (ALP) mRNA binds to and is stabilized by vimentin.

Two proteins with enzymatic properties were identified: Probable imidazolonepropionase (Q9DBA8, unique to zirconia after 7 days of culture), and N-alpha-acetyltransferase 20 (P61600, identified exclusively on Anod Ti at the 14th day). The first is involved in step 3 of the subpathway that synthesizes N-formimidoyl-L-glutamate from L-histidine. The latter is responsible for N-terminal peptidyl-methionine acetylation and is required for maintaining the structure and function of actomyosin fibers and for proper cellular migration. In a recent work by Fernandes et al. (2018)[24], it was demonstrated that ECM remodeling is a pre-requisite to pre-osteoblast phenotype response to zirconia, involving a cascade of signaling molecules related to cellular anchoring.

One of the categories with the highest percentage of associated genes in the ClueGo analysis was glycogen catabolic process. On zirconia, two proteins related to energy metabolism had a lower expression when compared to that of cp-Ti at the 7$^{th}$ and at the 14$^{th}$ day, but at the 21th day they became equalized. One protein was up-regulated on Anod Ti after 7 days of culture when compared to cp-Ti, but there was no difference in energy metabolism proteins between them afterwards. significant biological process mentioned was glycogen catabolic process.

Alpha-1,4 glucan phosphorylase was down-regulated on zirconia on the 7$^{th}$ day, while Glycogen phosphorylase brain form was up-regulated on Anod Ti on the same day and down-regulated on zirconia on the 14$^{th}$ day. Phosphorylases are allosteric enzymes of glycogenolysis, participating on the carbohydrate metabolism, being found in the extracellular region or secreted by the cells. In our data, glycogen phosphorylase brain form was indirectly associated with High mobility group nucleosome-binding domain-containing protein 5 (Q9JL35), found on Anod Ti on the 14$^{th}$ day, through a common link to 14–3-3 protein epsilon (P62259).

These results suggest that the earlier cellular metabolism on zirconia is somehow slower when compared to that observed on cp-Ti and Anod Ti, maybe associated with the smoother surface. On the other hand, Anod Ti seems to require a higher level of energy at initial times. Perhaps its chemical composition, enriched with Ca, P and Mg, helps promoting the cellular proliferation typical of that phase. No articles were found in the literature specifically describing these two proteins and their relation to osteoblasts metabolism, but Komarova et al (2000)[25] suggested that the glycolytic component of energy generation in mature osteoblasts may play a key role in adapting to transient challenges such as changes in either $O_2$ supply to bone or increases in transient demands for energy.

Another significant biological process mentioned in the ClueGo analysis was the positive regulation of collagen biosynthetic process. Collagens, as is well known, are the main structural components of the ECM, focus of our study.

In spite of the great variety of studies found within the contemporary bio-medical literature regarding proteomics and biomaterials, as evidenced by the recent review by Othman et al (2018)[26], none was focused on describing the ECM proteins expressed differentially on three different biomaterials The novelty of the processes used to limit the number of analyzed proteins, comprising decellularization followed by ECM collection by scrapping, improves the validity of our data. Proteomic analysis of whole cell lysates usually involve hundreds of proteins, while in our work, only 24 proteins were found

uniquely or differentially expressed. Our results contribute to the elucidation of osteoblastic ECM composition along time and the effect biomaterial surfaces cause in the mineralization process. Further studies are needed to confirm the described temporal changes and the effect the mentioned proteins have on osseointegration.

## Conclusions

The small number of identified proteins demonstrates that the chosen decellularization process was effective at reducing the proteome dataset. Typical ECM proteins were expressed and regulated equally on the three biomaterials tested. Some proteins related to bone development, like TGF-β3, were found exclusively on cp-Ti on the 21$^{st}$ day. Alpha-1_4 glucan phosphorylase and Glycogen phosphorylase brain form, both proteins involved in metabolic processes, were down-regulated on zirconia after 7 and 14 days of culture, and up-regulated on Anod Ti on the 7$^{th}$ day, suggesting the influence of material surface roughness and chemical composition on energy metabolism. Our results are the first obtained by isolating the ECM generated by osteoblasts over implant biomaterials and reveal new insights regarding osseointegration and how material surfaces affect this process.

## Acknowledgments

The authors thank Centro Integrado de Pesquisa (CIP) and the Biochemistry Laboratory of Bauru School of Dentistry, USP for providing research facilities. Special thanks to Prof. Dr. Luís Augusto Rocha, Departamento de Física, Faculdade de Ciências - FC/UNESP Bauru, for the donation of the commercially pure and anodized titanium samples, and to Mileni da Silva Fernandes for excellent assistance on mass spectrometry.

## References

1. Martins R, Cestari TM, Arantes RVN, et al. Osseointegration of zirconia and titanium implants in a rabbit tibiae model evaluated by microtomography, histomorphometry and fluorochrome labeling analyses. *J Periodontal Res*. 2018;53(2):210-221. doi:10.1111/jre.12508

2. Özkurt Z, Kazazoğlu E. Zirconia dental implants: a literature review. *J Oral Implantol*. 2011;37(3):367-376. doi:10.1563/AAID-JOI-D-09-00079

3. Alves a C, Oliveira F, Wenger F, Ponthiaux P, Celis J-P, Rocha L a. Tribocorrosion behaviour of anodic treated titanium surfaces intended for dental implants. *J Phys D Appl Phys*. 2013;46(40):404001. doi:10.1088/0022-3727/46/40/404001

4. Meyer U, Büchter A, Wiesmann HP, Joos U, Jones DB. Basic reactions of osteoblasts on structured material surfaces. *Eur Cell Mater*. 2005;9:39-49.

5. Mouw JK, Ou G, Weaver VM. Extracellular matrix assembly: A multiscale deconstruction. *Nat Rev Mol Cell Biol*. 2014;15(12):771-785. doi:10.1038/nrm3902

6. Grzesiak J, Śmieszek A, Marycz K. Ultrastructural changes during osteogenic differentiation in mesenchymal stromal cells cultured in alginate hydrogel. *Cell Biosci*. 2017;7:2.

doi:10.1186/s13578-016-0128-0

7. Xiao Z, Camalier CE, Nagashima K, et al. Analysis of the extracellular matrix vesicle proteome in mineralizing osteoblasts. *J Cell Physiol*. 2007;210(2):325-335. doi:10.1002/jcp.20826

8. Xu J, Khor KA, Sui J, Zhang J, Tan TL, Chen WN. Comparative proteomics profile of osteoblasts cultured on dissimilar hydroxyapatite biomaterials: an iTRAQ-coupled 2-D LC-MS/MS analysis. *Proteomics*. 2008;8(20):4249-4258. doi:10.1002/pmic.200800103

9. Rashid ST, Humphries JD, Byron A, et al. Proteomic analysis of extracellular matrix from the hepatic stellate cell line LX-2 identifies CYR61 and Wnt-5a as novel constituents of fibrotic liver. *J Proteome Res*. 2012;11(8):4052-4064. doi:10.1021/pr3000927

10. Ribeiro AR, Oliveira F, Boldrini LC, et al. Micro-arc oxidation as a tool to develop multifunctional calcium-rich surfaces for dental implant applications. *Mater Sci Eng C*. 2015;54:196-206. doi:10.1016/j.msec.2015.05.012

11. H. Sudo, H. A. Kodama, Y. Amagai, S. Yamamoto SK. In Vitro Differentiation and Calcification in a New Clonal Osteogenic Cell Line Derived from Newborn Mouse Calvaria. http://jcb.rupress.org/content/96/1/191.full.pdf. Accessed March 16, 2015.

12. Dionizio AS, Melo CGS, Sabino-Arias IT, et al. Chronic treatment with fluoride affects the jejunum: insights from proteomics and enteric innervation analysis. *Sci Rep*. 2018;8(1):1-12. doi:10.1038/s41598-018-21533-4

13. Marumoto A, Milani R, da Silva RA, et al. Phosphoproteome analysis reveals a critical role for hedgehog signalling in osteoblast morphological transitions. *Bone*. 2017;103:55-63. doi:10.1016/j.bone.2017.06.012

14. Lin Y, Huang Y, He J, Chen F, He Y, Zhang W. Role of Hedgehog–Gli1 signaling in the enhanced proliferation and differentiation of MG63 cells enabled by hierarchical micro-/nanotextured topography. *Int J Nanomedicine*. 2017;Volume 12:3267-3280. doi:10.2147/IJN.S135045

15. Xiong L, Jung J-U, Wu H, et al. Lrp4 in osteoblasts suppresses bone formation and promotes osteoclastogenesis and bone resorption. *Proc Natl Acad Sci*. 2015;112(11):3487-3492. doi:10.1073/pnas.1419714112

16. Sophocleous A, Marino S, Kabir D, Ralston SH, Idris AI. Combined deficiency of the Cnr1 and Cnr2 receptors protects against age-related bone loss by osteoclast inhibition. *Aging Cell*. 2017;16(5):1051-1061. doi:10.1111/acel.12638

17. Wang W, Olson D, Liang G, et al. Collagen XXIV (Col24a1) promotes osteoblastic differentiation and mineralization through TGF-β/smads signaling pathway. *Int J Biol Sci*. 2012;8(10):1310-1322. doi:10.7150/ijbs.5136

18. Deng M, Mei T, Hou T, et al. TGFβ3 recruits endogenous mesenchymal stem cells to initiate bone regeneration. *Stem Cell Res Ther*. 2017;8(1):1-12. doi:10.1186/s13287-017-0693-0

19. Valta MP, Hentunen T, Qu Q, et al. Regulation of osteoblast differentiation: A novel function for fibroblast growth factor 8. *Endocrinology*. 2006;147(5):2171-2182. doi:10.1210/en.2005-1502

20. Lin J-M, Callon KE, Lin J-S, et al. Actions of fibroblast growth factor-8 in bone cells in vitro. *Am J Physiol Metab*. 2009;297(1):E142-E150. doi:10.1152/ajpendo.90743.2008

21. Lian N, Wang W, Li L, Elefteriou F, Yang X. Vimentin Inhibits ATF4-mediated Osteocalcin Transcription and Osteoblast Differentiation. *J Biol Chem*. 2009;284(44):30518-30525. doi:10.1074/jbc.M109.052373

22. Lian N, Lin T, Liu W, et al. Transforming growth factor β suppresses osteoblast differentiation via the vimentin activating transcription factor 4 (ATF4) axis. *J Biol Chem*. 2012;287(43):35975-35984. doi:10.1074/jbc.M112.372458

23. Schmidt Y, Biniossek M, Stark GB, Finkenzeller G, Simunovic F. Osteoblastic alkaline phosphatase mRNA is stabilized by binding to vimentin intermediary filaments. *Biol Chem*. 2015;396(3). doi:10.1515/hsz-2014-0274

24. da Costa Fernandes CJ, Ferreira MR, Bezerra FJB, Zambuzzi WF. Zirconia stimulates ECM-remodeling as a prerequisite to pre-osteoblast adhesion/proliferation by possible interference with cellular anchorage. *J Mater Sci Mater Med*. 2018;29(4). doi:10.1007/s10856-018-6041-9

25. Komarova S V., Ataullakhanov FI, Globus RK. Bioenergetics and mitochondrial transmembrane potential during differentiation of cultured osteoblasts. *Am J Physiol Physiol*. 2000;279(4):C1220-C1229. doi:10.1152/ajpcell.2000.279.4.C1220

26. Othman Z, Cillero Pastor B, van Rijt S, Habibovic P. Understanding interactions between biomaterials and biological systems using proteomics. *Biomaterials*. 2018;167:191-204. doi:10.1016/j.biomaterials.2018.03.020

# *3 Discussion*

## 3 DISCUSSION

Dental implant failures cause patient discomfort and bone loss is often clinically observed. It is therefore important to assure good osseointegration capability and appropriate mechanical properties to withstand the masticatory pressures. Titanium is the gold standard for dental implant industry, but new materials as well as surface treatments have been investigated aiming at a long-lasting performance allied to improved aesthetics. In this context, we decided to compare three different biomaterials: commercially pure titanium (cp-Ti grade 2), anodized titanium surface and yttria stabilized zirconia (Y-TZP) in a longitudinal study.

Surface treatments like polishing, sandblasting, acid etching, coatings, nanotextures and biofunctionalization have been proposed and tested over titanium and zirconia (12,22–26). As mentioned earlier, the anodization process improves cell attachment and proliferation (27), but less work has been done on the final steps of osseointegration and the bone quality obtained.

Techniques used to evaluate mineralization includes von Kossa staining (28), colorimetric assays based on alizarin red staining (29), or EDX (30). Direct fluorescent labelling of hydroxyapatite crystals by calcein was used for visualization (11,16), fluorometric quantitation (10,31) or nodule area measurement (12,32), but no work has been published measuring the mineralization volume based upon confocal 3D imaging.

When comparing anodized titanium (TiUnite®), machined titanium (Ti-m), sandblasted and acid-etched zirconia (TZP- proc), and machined zirconia (TZP-A-m), Kohal et al. (2013)(23) observed contradictory results. Similar to our results, the cell responses to zirconia surfaces were comparable to those obtained over titanium, but in the *in vivo* experiment TZP-proc performed worse than a standard titanium implant surface modification. Hempel et al. (2010) also compared titanium and zirconia with two surface modifications, and significantly higher calcium accumulation was obtained on both zirconia surfaces when compared with titanium (33).

In our work, cp-Ti was the roughest surface, while zirconia was the smoothest. Notwithstanding, the amount of mineralization obtained over both materials were equivalent. Our results suggest that roughness alone may not be a determining parameter concerning cell behavior, agreeing with the conclusion presented by Setzer

et al. (2008) (29). Besides, this result strengthens the use of zirconia in the clinic by suggesting that both materials would present a similar osseointegration. On the other hand, anodized titanium presented a greater mineralization volume compared to the other two biomaterials, probably due to its chemical composition or porosity, as suggested in the works of Alves et al. (24,34).

Also, Anselme et al. (35) stated that there was a negative correlation between roughness and cell adhesion and proliferation, yet the roughness organization and surface chemical composition were relevant, as it seems to be the case for anodized titanium in our work.

In the present study, all biomaterials showed a good proliferation of MC3T3 cells. It has been reported that osteoblasts undergo shape changes as they differentiate: the cell loses its flattened, elongated shape and adopts a cuboidal morphology. The actin restructuring observed after 14 days of culture is in agreement with the results shown in previous study by Titushkin et al. (2007)(36). In a study on the elasticity of the extracellular matrix, Meng et al. (2009), stated that only mineralizing osteoblasts have the cytoskeleton remodeled when compared to the inactive ones, and also that mineralization requires a correct and completely developed ECM to occur (37).

TAKAI et al. (2005) cultivated osteoblasts for 1 hour on glass coated or not by collagen type I, fibronectin, vitronectin, poly-L-lysine, and fetal bovine serum to assess the influence of the extracellular matrix proteins on the cellular elasticity and cytoskeleton. In adhesion processes mediated by integrins (in the case of collagen type I, fibronectin, vitronectin and fetal bovine serum) the cytoskeleton proved more robust and the cells were firmer. On the contrary, the cells grown on glass and poly-L-lysine, where adhesion occurs by non-specific connections, presented the cytoskeleton with fewer actin fibers and smaller elastic modules (38).

Among many other functions like adhesion (39), migration and cellular morphology, the cytoskeleton is responsible for vesicle transport. Osteoblasts release matrix vesicles (MVs), which are the initial sites where crystals of apatite bone mineral are formed (40).

Many efforts have been undertaken to understand the process and mechanism of MV formation and release. Some results have suggested that the MV release is mediated by the actin cytoskeleton. A correlation between the release of MVs and changes in cellular actin distribution has been reported by Hale et al. (41). Furthermore,

actin microfilament disassembly is involved in the mechanism of MV formation, as Thouverey et al. demonstrated (42).

Our current data have shown a weak inverse correlation between mineralization and actin cytoskeleton volumes, reinforcing the role of the actin fibers depolymerization in the formation of MVs. This result makes it of interest to investigate other techniques like fluorescent colocalization or proteomics to further elucidate this mechanism.

Much of the pivotal role ECM proteins play in osseointegration remains unclear. As previously mentioned, ECM components participate in cellular signaling, besides providing structural support. Many research efforts are focused on ECM description, trying to elucidate its complex composition and dynamical behavior (17). We employed a proteomic approach to evaluate differences in ECM protein expression from osteoblasts cultivated on three different implant surfaces, and how it changes over time.

Our results revealed that the great majority of the ECM proteins are expressed and regulated equally on the three biomaterials tested, albeit distinct chemical compositions and surface roughness. Some proteins identified were uniquely found on a biomaterial at certain time points, whereas only two proteins were up or down-regulated.

Two enzymatic proteins were identified: Probable imidazolonepropionase (Q9DBA8, unique to zirconia after 7 days of culture), and N-alpha-acetyltransferase 20 (P61600, identified exclusively on Anod Ti at the 14th day). The first is involved in step 3 of the subpathway that synthesizes N-formimidoyl-L-glutamate from L-histidine. The latter is responsible for N-terminal peptidyl-methionine acetylation and is required for maintaining the structure and function of actomyosin fibers and for proper cellular migration. It has been demonstrated that ECM remodeling is a pre-requisite to pre-osteoblast phenotype response in a recent work by Da Costa Fernandes et al. (2018). The cellular response to zirconia involved a cascade of signaling molecules related to cellular anchoring (43). The fact that enzymes were identified in this work certifies that the samples were properly handled, as they are very sensitive to heat.

Some proteins identified in the collected ECMs are classified as membrane receptors and growth factors or associated to molecular signaling pathways, normally found in the extracellular region. B9 domain-containing protein 1 (Q9R1S0) is required for sonic hedgehog/Shh signaling and was uniquely found on zirconia on the 7$^{th}$ day. The role of the Hedgehog-Gli1 pathway in the response of osteoblasts to different

titanium topographies was evaluated by Lin (2017), and on the nanostructured surface studied, the mRNA expression of Sonic hedgehog (Shh) was higher when compared to that on the smooth and microstructured surfaces.(44). In our work, the zirconia surface presents irregularities in the nanoscale, which may have caused a similar effect.

Breakpoint cluster region protein was unique to zirconia at 7$^{th}$ day. Being a GTPase-activating protein for the GTPases of the Rho family, it is involved in the regulation of Rho protein signal transduction, negative regulation of cell migration, regulation of cell cycle, actin cytoskeleton organization and intracellular protein transmembrane transport, among other functions. In our work, this protein was found associated with Cell cycle progression protein 1 (Q640L3). The latter is a membrane protein involved in positive regulation of cell cycle and cell proliferation, acting as an assembly platform for Rho protein signaling complexes.

Low-density lipoprotein receptor-related protein 4 (Q8VI56, Lrp4) was uniquely identified on zirconia at the 7$^{th}$ day. In this work, it was associated with Agrin, known to induce an increase in cytoplasmic calcium ions, specifically modulating calcium ion homeostasis in neurons. Xiong et al (2015)(45) identified Lrp4 as a critical player in bone mass homeostasis, acting as a receptor of sclerostin to inhibit Wnt/β-catenin signaling and bone formation.

The work of Sophocleous et al. (2017) indicates that Cannabinoid receptor 2 (P47936, Cnr2) plays a role in regulating bone mass and bone cell activity. Combined deficiency of the Cnr1 and Cnr2 receptors in female mice protects against age-related bone loss due to a reduction in osteoclast number when compared with wild-type (49). Our results show Cnr2 uniquely expressed on cp-Ti after 21 days of culture, during the mineralization phase.

Identified only on cp-Ti at the 21st day, transforming growth factor beta-3 (Q91YU7, TGF-β3) is typically found in the extracellular region. Among other functions, it participates in the positive regulation of bone mineralization and positive regulation of collagen biosynthetic process. In a very elegant study of Wang et al (2012)(50), the relations between collagen XXIV, TGF-β e Smad were demonstrated in MC3T3 cells. Interestingly, a recent work by Deng (2017)(51) reports that TGFβ3 could recruit MSCs to initiate bone regeneration.

Another grow factor identified in this work, typical of the extracellular region, Fibroblast growth factor 8 (P37237) was found exclusively expressed on cp-Ti at the

21st day. It plays an important role in the regulation of embryonic development, cell proliferation, cell differentiation and cell migration. Valta et al. (2006) showed that besides inducing osteoblast differentiation, FGF-8 stimulates the proliferation of cultured mouse bone marrow cells efficiently and induced their early stage differentiation (52). The stimulatory effects of FGF-8 on osteoblast proliferation in primary osteoblast cultures was also proved in a study by Lin et al (2009) , while in long-term cultures of osteoblasts, nodule formation was inhibited (53).

Cytoskeleton associated proteins like centriolin (A2AL36, unique to Anod Ti at the 7$^{th}$ day), MAP7 domain-containing protein 2 (A2AG50, unique to Anod Ti at the 14$^{th}$ day), and vimentin were also identified. Vimentins are class-III intermediate filaments, localized in the extracellular matrix or as part of the cytoskeleton. According to Gene Ontology, it is involved in the positive regulation of collagen biosynthetic process and SMAD protein signal transduction. In this work vimentin was identified as exclusive for the cp-Ti group after 21 days of culture.

One association between osteoblasts and vimentin was described by Lian et al. (2009) where vimentin inhibited differentiation in immature osteoblasts by interacting with Activating transcription factor 4 (ATF4) (46). Later, Lian et al. (2012) described this process in detail, stating that TGF-β stimulates vimentin production, leading to suppression of ATF4-dependent osteocalcin (Ocn) transcription and osteoblast differentiation (47). Schmidt et al. (2015) demonstrated that alkaline phosphatase (ALP) mRNA binds to and is stabilized by vimentin (48).

Curiously, various proteins related to bone remodeling were found exclusively expressed on cp-Ti at the 21$^{st}$ day. At the same time point, zirconia presented the same amount of mineralization as cp-Ti, while Anod Ti had a greater amount of mineralization. So why those proteins weren´t identified on zirconia and Anod Ti? Perhaps on both materials the cellular cycle is more advanced when compared to cp-Ti. This hypothesis could only be checked in a study where the time points were closer.

One of the categories with the highest percentage of associated genes in the ClueGo analysis was glycogen catabolic process. On zirconia, two proteins related to energy metabolism had a lower expression when compared to that of cp-Ti at the 7$^{th}$ and at the 14$^{th}$ day, but at the 21th day they became equalized. One protein was up-regulated on Anod Ti after 7 days of culture when compared to cp-Ti, but there was no difference in energy metabolism proteins between them afterwards.

Alpha-1,4 glucan phosphorylase was down-regulated on zirconia on the 7th day, while Glycogen phosphorylase brain form was up-regulated on Anod Ti on the same day and down-regulated on zirconia on the 14th day. Phosphorylases are allosteric enzymes of glycogenolysis, participating on the carbohydrate metabolism, being found in the extracellular region or secreted by the cells. In our data, glycogen phosphorylase brain form was indirectly associated with High mobility group nucleosome-binding domain-containing protein 5 (Q9JL35), found on Anod Ti on the 14th day, through a common link to 14–3-3 protein epsilon (P62259).

These results suggest that the early cellular metabolism on zirconia is somehow slower when compared to that observed on cp-Ti and Anod Ti, maybe associated with the smoother surface. On the other hand, Anod Ti seems to require a higher level of energy at initial times. Perhaps its chemical composition, enriched with Ca, P and Mg, helps promoting the cellular proliferation typical of that phase. No articles were found in the literature specifically describing these two proteins and their relation to osteoblasts metabolism, but Komarova et al. (2000) suggested that the glycolytic component of energy generation in mature osteoblasts may play a key role in adapting to transient challenges such as changes in either $O_2$ supply to bone or increases in transient demands for energy (54).

Another significant biological process appointed in the ClueGo analysis was the positive regulation of collagen biosynthetic process. Collagens, as is well known, are the main structural components of the ECM, focus of our study.

In spite of the great variety of studies found within the contemporary bio-medical literature regarding proteomics and biomaterials, as evidenced by the recent review by Othman et al. (2018) (55), none was focused on describing the ECM proteins expressed differentially on three different biomaterials. The novelty of the processes used to limit the number of analyzed proteins, comprising decellularization followed by ECM collection by scrapping, improves the validity of our data. Proteomic analysis of whole cell lysates usually involve hundreds of proteins, while in our work, only 24 proteins were found uniquely or differentially expressed. Our results contribute to the comprehension of the complex relationships between ECM composition, cytoskeleton remodeling and mineralizing capacity of osteoblastic cells along time and the effect biomaterial surfaces cause in this process. Further studies are needed to confirm the temporal changes and the implications of the uniquely expressed proteins mentioned.

# *4 Conclusions*

# 4 CONCLUSIONS

The greater mineralization obtained over the anodized titanium after 21 days demonstrated an improved response provided by the surface modification. The amount of mineral deposition obtained over zirconia was equivalent to that of cp-Ti, which favors the use of zirconia in the clinic. An inverse correlation between mineralization and cytoskeleton volume has been shown, strengthening the hypothesis of actin fibers depolymerization related to mineral deposits through MVs. The innovative volume quantification technique adopted was useful in providing information about the cellular status and biomaterial performance in terms of osseointegration.

The small number of identified proteins demonstrates that the chosen decellularization process was effective at reducing the proteome dataset. Typical ECM proteins were expressed and regulated equally on the three biomaterials tested. Some proteins related to bone development, like TGF-β3, were found exclusively on cp-Ti on the 21$^{st}$ day. Alpha-1_4 glucan phosphorylase and Glycogen phosphorylase brain form, both proteins involved in metabolic processes, were down-regulated on zirconia after 7 and 14 days of culture, and up-regulated on Anod Ti on the 7$^{th}$ day, suggesting the influence of material surface roughness and chemical composition on energy generation. Our results are the first obtained by isolating the ECM generated by osteoblasts over implant biomaterials and reveal new insights regarding osseointegration and how material surfaces affect this process.

# *References*

## REFERENCES

1. Alves a C, Oliveira F, Wenger F, Ponthiaux P, Celis J-P, Rocha L a. Tribocorrosion behaviour of anodic treated titanium surfaces intended for dental implants. J Phys D Appl Phys [Internet]. 2013 Oct 9;46(40):404001. Available from: http://stacks.iop.org/0022-3727/46/i=40/a=404001?key=crossref.798810ece9bd05ce3c9a76ad76114463

2. Ribeiro AR, Gemini-Piperni S, Travassos R, Lemgruber L, Silva RC, Rossi AL, et al. Trojan-Like Internalization of Anatase Titanium Dioxide Nanoparticles by Human Osteoblast Cells. Sci Rep [Internet]. 2016 Mar 29 [cited 2017 Jan 20];6:23615. Available from: http://www.nature.com/articles/srep23615

3. Özkurt Z, Kazazoğlu E. Zirconia dental implants: a literature review. J Oral Implantol [Internet]. 2011 Jun [cited 2014 Feb 4];37(3):367–76. Available from: http://www.ncbi.nlm.nih.gov/pubmed/20545529

4. Ribeiro AR, Oliveira F, Boldrini LC, Leite PE, Falagan-Lotsch P, Linhares ABR, et al. Micro-arc oxidation as a tool to develop multifunctional calcium-rich surfaces for dental implant applications. Mater Sci Eng C. 2015;54:196–206.

5. Oliveira FG, Ribeiro AR, Perez G, Archanjo BS, Gouvea CP, Araújo JR, et al. Understanding growth mechanisms and tribocorrosion behaviour of porous TiO2 anodic films containing calcium, phosphorous and magnesium. Appl Surf Sci. 2015;341:1–12.

6. Hisbergues M, Vendeville S, Vendeville P. Zirconia: Established facts and perspectives for a biomaterial in dental implantology. J Biomed Mater Res B Appl Biomater [Internet]. 2009 Mar [cited 2014 Jan 31];88(2):519–29. Available from: http://www.ncbi.nlm.nih.gov/pubmed/18561291

7. Soon G, Pingguan-Murphy B, Lai KW, Akbar SA. Review of zirconia-based bioceramic: Surface modification and cellular response. Vol. 42, Ceramics International. 2016. p. 12543–55.

8. Assal P. The Osseointegration of Zirconia Dental Implants. … fur Zahnmedizin= Rev Mens suisse d'odonto- … [Internet]. 2012 [cited 2014 Feb 4]; Available from: http://europepmc.org/abstract/MED/23965893

9. Martins R, Cestari TM, Arantes RVN, Santos PS, Taga R, Carbonari MJ, et al. Osseointegration of zirconia and titanium implants in a rabbit tibiae model evaluated by microtomography, histomorphometry and fluorochrome labeling

analyses. J Periodontal Res. 2018;53(2):210–21.

10. Uchimura E, Machida H, Kotobuki N, Kihara T, Kitamura S, Ikeuchi M, et al. In-situ visualization and quantification of mineralization of cultured osteogenetic cells. Calcif Tissue Int [Internet]. 2003 Dec [cited 2014 Jan 4];73(6):575–83. Available from: http://www.ncbi.nlm.nih.gov/pubmed/12958691

11. Ahmad M, Mccarthy M, Gronowicz G. An in vitro model for mineralization of human osteoblast-like cells on implant materials. 1999;20:211–20.

12. de Oliveira PT, Zalzal SF, Beloti MM, Rosa AL, Nanci A. Enhancement of in vitro osteogenesis on titanium by chemically produced nanotopography. J Biomed Mater Res A [Internet]. 2007 Mar 1 [cited 2014 Jan 16];80(3):554–64. Available from: http://www.ncbi.nlm.nih.gov/pubmed/17031821

13. Hempel U, Hefti T, Kalbacova M, Wolf-Brandstetter C, Dieter P, Schlottig F. Response of osteoblast-like SAOS-2 cells to zirconia ceramics with different surface topographies. Clin Oral Implants Res [Internet]. 2010 Mar [cited 2014 Jan 29];21(2):174–81. Available from: http://www.ncbi.nlm.nih.gov/pubmed/19709059

14. Meyer U, Büchter A, Wiesmann HP, Joos U, Jones DB. Basic reactions of osteoblasts on structured material surfaces. Eur Cell Mater. 2005;9:39–49.

15. Lee K, Yeung H. Application of Laser Scanning Confocal Microscopy in Musculoskeletal Research.

16. Kihara T, Oshima A, Hirose M, Ohgushi H. Three-dimensional visualization analysis of in vitro cultured bone fabricated by rat marrow mesenchymal stem cells. Biochem Biophys Res Commun [Internet]. 2004 Apr 9 [cited 2014 Jan 4];316(3):943–8. Available from: http://www.ncbi.nlm.nih.gov/pubmed/15033493

17. Mouw JK, Ou G, Weaver VM. Extracellular matrix assembly: A multiscale deconstruction [Internet]. Vol. 15, Nature Reviews Molecular Cell Biology. 2014 [cited 2017 Jun 21]. p. 771–85. Available from: https://www.nature.com/nrm/journal/v15/n12/pdf/nrm3902.pdf

18. Grzesiak J, Śmieszek A, Marycz K. Ultrastructural changes during osteogenic differentiation in mesenchymal stromal cells cultured in alginate hydrogel. Cell Biosci [Internet]. 2017 [cited 2017 Jan 17];7:2. Available from: http://www.ncbi.nlm.nih.gov/pubmed/28066541

19. Xiao Z, Camalier CE, Nagashima K, Chan KC, Lucas DA, de la Cruz MJ, et al. Analysis of the extracellular matrix vesicle proteome in mineralizing osteoblasts. J Cell Physiol [Internet]. 2007 Feb 1 [cited 2016 Feb 2];210(2):325–35. Available from: http://onlinelibrary.wiley.com/doi/10.1002/jcp.20826/full

20. Xu J, Khor KA, Sui J, Zhang J, Tan TL, Chen WN. Comparative proteomics profile of osteoblasts cultured on dissimilar hydroxyapatite biomaterials: an iTRAQ-coupled 2-D LC-MS/MS analysis. Proteomics [Internet]. 2008 Oct [cited 2016 Feb 2];8(20):4249–58. Available from: http://www.ncbi.nlm.nih.gov/pubmed/18924181

21. Rashid ST, Humphries JD, Byron A, Dhar A, Askari JA, Selley JN, et al. Proteomic analysis of extracellular matrix from the hepatic stellate cell line LX-2 identifies CYR61 and Wnt-5a as novel constituents of fibrotic liver. J Proteome Res [Internet]. 2012 Aug 3 [cited 2016 Jun 15];11(8):4052–64. Available from: http://www.ncbi.nlm.nih.gov/pubmed/22694338

22. Kou W, Akasaka T, Watari F, Sjögren G. An in vitro evaluation of the biological effects of carbon nanotube-coated dental zirconia. ISRN Dent [Internet]. 2013 Jan;2013:296727. Available from: http://www.pubmedcentral.nih.gov/articlerender.fcgi?artid=3762083&tool=pmcentrez&rendertype=abstract

23. Kohal RJ, Bächle M, Att W, Chaar S, Altmann B, Renz A, et al. Osteoblast and bone tissue response to surface modified zirconia and titanium implant materials. Dent Mater [Internet]. 2013 Jul [cited 2014 Jan 27];29(7):763–76. Available from: http://www.ncbi.nlm.nih.gov/pubmed/23669198

24. Alves SA, Ribeiro AR, Gemini-Piperni S, Silva RC, Saraiva AM, Leite PE, et al. $TiO_2$ nanotubes enriched with calcium, phosphorous and zinc: promising bio-selective functional surfaces for osseointegrated titanium implants. RSC Adv [Internet]. 2017;7(78):49720–38. Available from: http://xlink.rsc.org/?DOI=C7RA08263K

25. Hanawa T. A comprehensive review of techniques for biofunctionalization of titanium. J Periodontal Implant Sci [Internet]. 2011 Dec [cited 2014 Feb 25];41(6):263–72. Available from: http://www.pubmedcentral.nih.gov/articlerender.fcgi?artid=3259234&tool=pmcentrez&rendertype=abstract

26. Depprich R, Ommerborn M, Zipprich H, Naujoks C, Handschel J, Wiesmann H-P, et al. Behavior of osteoblastic cells cultured on titanium and structured zirconia surfaces. Head Face Med. 2008;4:29.

27. Yao C, Slamovich EB, Webster TJ. Enhanced osteoblast functions on anodized titanium with nanotube-like structures. J Biomed Mater Res - Part A. 2008;85(1):157–66.

28. Kwun IS, Cho YE, Lomeda RAR, Shin HI, Choi JY, Kang YH, et al. Zinc deficiency suppresses matrix mineralization and retards osteogenesis transiently with catch-up possibly through Runx 2 modulation. Bone [Internet]. 2010;46(3):732–41. Available from: http://dx.doi.org/10.1016/j.bone.2009.11.003

29. Setzer B, Bächle M, Metzger MC, Kohal RJ. The gene-expression and phenotypic response of hFOB 1.19 osteoblasts to surface-modified titanium and zirconia. Biomaterials [Internet]. 2009 Mar [cited 2014 Jan 29];30(6):979–90. Available from: http://www.ncbi.nlm.nih.gov/pubmed/19027946

30. Markwardt J, Friedrichs J, Werner C, Davids A, Weise H, Lesche R, et al. Experimental study on the behavior of primary human osteoblasts on laser-cused pure titanium surfaces. J Biomed Mater Res - Part A. 2014;102(5):1422–30.

31. Hale L V, Ma YF, Santerre RF. Semi-quantitative fluorescence analysis of calcein binding as a measurement of in vitro mineralization. Calcif Tissue Int [Internet]. 2000 Jul [cited 2014 Jan 13];67(1):80–4. Available from: http://link.springer.com/article/10.1007/s00223001101

32. Bosetti M, Leigheb M, Brooks RA, Boccafoschi F, Cannas MF. Regulation of osteoblast and osteoclast functions by FGF-6. J Cell Physiol. 2010;225(2):466–71.

33. Hempel U, Hefti T, Kalbacova M, Wolf-Brandstetter C, Dieter P, Schlottig F. Response of osteoblast-like SAOS-2 cells to zirconia ceramics with different surface topographies. Clin Oral Implants Res [Internet]. 2010 Mar [cited 2014 Jan 29];21(2):174–81. Available from: http://www.ncbi.nlm.nih.gov/pubmed/19709059

34. Alves SA, Patel SB, Sukotjo C, Mathew MT, Filho PN, Celis JP, et al. Synthesis of calcium-phosphorous doped TiO2nanotubes by anodization and reverse polarization: A promising strategy for an efficient biofunctional implant surface. Appl Surf Sci. 2017;399(December):682–701.

35. Anselme K, Linez P, Bigerelle M, Le Maguer D, Le Maguer A, Hardouin P, et al. The relative influence of the topography and chemistry of TiAl6V4 surfaces on osteoblastic cell behaviour. Biomaterials. 2000;21:1567–77.

36. Titushkin I, Cho M. Modulation of cellular mechanics during osteogenic differentiation of human mesenchymal stem cells. Biophys J [Internet]. 2007 Nov 15 [cited 2013 Dec 16];93(10):3693–702. Available from: http://www.pubmedcentral.nih.gov/articlerender.fcgi?artid=2072058&tool=pmcentrez&rendertype=abstract

37. Meng Y, Qin Y-X, DiMasi E, Ba X, Rafailovich M, Pernodet N. Biomineralization of a self-assembled extracellular matrix for bone tissue engineering. Tissue Eng Part A [Internet]. 2009 Feb;15(2):355–66. Available from: http://www.pubmedcentral.nih.gov/articlerender.fcgi?artid=2782659&tool=pmcentrez&rendertype=abstract

38. Takai E, Costa KD, Shaheen A, Hung CT, Guo XE. Osteoblast Elastic Modulus Measured by Atomic Force Microscopy Is Substrate Dependent. Ann Biomed Eng [Internet]. 2005 Jul [cited 2013 Dec 17];33(7):963–71. Available from: http://link.springer.com/10.1007/s10439-005-3555-3

39. Zambuzzi WF, Bruni-Cardoso A, Granjeiro JM, Peppelenbosch MP, De Carvalho HF, Aoyama H, et al. On the road to understanding of the osteoblast adhesion: Cytoskeleton organization is rearranged by distinct signaling pathways. J Cell Biochem. 2009;108(1):134–44.

40. Anderson HC. Matrix vesicles and calcification. Curr Rheumatol Rep. 2003;5(3):222–6.

41. Hale JE, Chin JE, Ishikawa Y, Paradiso PR, Wuthier RE. Correlation between distribution of cytoskeletal proteins and release of alkaline phosphatase-rich vesicles by epiphyseal chondrocytes in primary culture. Cell Motil. 1983;3(5):501–12.

42. Thouverey C, Strzelecka-Kiliszek A, Balcerzak M, Buchet R, Pikula S. Matrix vesicles originate from apical membrane microvilli of mineralizing osteoblast-like saos-2 cells. J Cell Biochem. 2009;106(1):127–38.

43. da Costa Fernandes CJ, Ferreira MR, Bezerra FJB, Zambuzzi WF. Zirconia stimulates ECM-remodeling as a prerequisite to pre-osteoblast adhesion/proliferation by possible interference with cellular anchorage. J Mater Sci Mater Med [Internet]. 2018;29(4). Available from: http://dx.doi.org/10.1007/s10856-018-6041-9

44. Lin Y, Huang Y, He J, Chen F, He Y, Zhang W. Role of Hedgehog–Gli1 signaling in the enhanced proliferation and differentiation of MG63 cells enabled by hierarchical micro-/nanotextured topography. Int J Nanomedicine [Internet]. 2017 Apr;Volume 12:3267–80. Available from:

https://www.dovepress.com/role-of-hedgehogndashgli1-signaling-in-the-enhanced-proliferation-and--peer-reviewed-article-IJN

45. Xiong L, Jung J-U, Wu H, Xia W-F, Pan J-X, Shen C, et al. Lrp4 in osteoblasts suppresses bone formation and promotes osteoclastogenesis and bone resorption. Proc Natl Acad Sci [Internet]. 2015;112(11):3487–92. Available from: http://www.pnas.org/lookup/doi/10.1073/pnas.1419714112

46. Lian N, Wang W, Li L, Elefteriou F, Yang X. Vimentin Inhibits ATF4-mediated Osteocalcin Transcription and Osteoblast Differentiation. J Biol Chem [Internet]. 2009 Oct 30;284(44):30518–25. Available from: http://www.jbc.org/lookup/doi/10.1074/jbc.M109.052373

47. Lian N, Lin T, Liu W, Wang W, Li N, Sun S, et al. Transforming growth factor β suppresses osteoblast differentiation via the vimentin activating transcription factor 4 (ATF4) axis. J Biol Chem. 2012;287(43):35975–84.

48. Schmidt Y, Biniossek M, Stark GB, Finkenzeller G, Simunovic F. Osteoblastic alkaline phosphatase mRNA is stabilized by binding to vimentin intermediary filaments. Biol Chem [Internet]. 2015 Jan 1;396(3). Available from: https://www.degruyter.com/view/j/bchm.2015.396.issue-3/hsz-2014-0274/hsz-2014-0274.xml

49. Sophocleous A, Marino S, Kabir D, Ralston SH, Idris AI. Combined deficiency of the Cnr1 and Cnr2 receptors protects against age-related bone loss by osteoclast inhibition. Aging Cell. 2017;16(5):1051–61.

50. Wang W, Olson D, Liang G, Franceschi RT, Li C, Wang B, et al. Collagen XXIV (Col24a1) promotes osteoblastic differentiation and mineralization through TGF-β/smads signaling pathway. Int J Biol Sci. 2012;8(10):1310–22.

51. Deng M, Mei T, Hou T, Luo K, Luo F, Yang A, et al. TGFβ3 recruits endogenous mesenchymal stem cells to initiate bone regeneration. Stem Cell Res Ther. 2017;8(1):1–12.

52. Valta MP, Hentunen T, Qu Q, Valve EM, Harjula A, Seppänen JA, et al. Regulation of osteoblast differentiation: A novel function for fibroblast growth factor 8. Endocrinology. 2006;147(5):2171–82.

53. Lin J-M, Callon KE, Lin J-S, Watson M, Empson V, Tong PC, et al. Actions of fibroblast growth factor-8 in bone cells in vitro. Am J Physiol Metab [Internet]. 2009;297(1):E142–50. Available from: http://www.physiology.org/doi/10.1152/ajpendo.90743.2008

54. Komarova S V., Ataullakhanov FI, Globus RK. Bioenergetics and mitochondrial transmembrane potential during differentiation of cultured osteoblasts. Am J Physiol Physiol [Internet]. 2000;279(4):C1220–9. Available from: http://www.physiology.org/doi/10.1152/ajpcell.2000.279.4.C1220

55. Othman Z, Cillero Pastor B, van Rijt S, Habibovic P. Understanding interactions between biomaterials and biological systems using proteomics. Biomaterials [Internet]. 2018 Jun;167:191–204. Available from: http://linkinghub.elsevier.com/retrieve/pii/S014296121830187X

# *Appendix*

## APPENDIX A – DECLARATION OF EXCLUSIVE USE OF ARTICLE IN THESIS

We hereby declare that we are aware of the article **On a novel method for evaluation of the mineralization process of osteoblasts on biomaterials surfaces** will be included in Thesis of the student Márcia Sirlene Zardin Graeff was not used and may not be used in other works of Graduate Programs at the Bauru School of Dentistry, University of São Paulo.

Bauru, June 6th, 2018.

Márcia Sirlene Zardin Graeff
Author

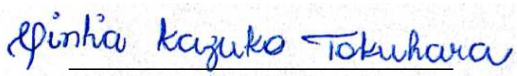

Cintia Kazuko Tokuhara
Author

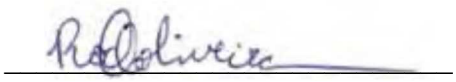

Rodrigo Cardoso de Oliveira
Author

**APPENDIX B – DECLARATION OF EXCLUSIVE USE OF ARTICLE IN THESIS**

We hereby declare that we are aware of the article **Longitudinal comparison of the ECM proteins from osteoblasts cultivated on different biomaterials** will be included in Thesis of the student Márcia Sirlene Zardin Graeff was not used and may not be used in other works of Graduate Programs at the Bauru School of Dentistry, University of São Paulo.

Bauru, June 6th, 2018.

Márcia Sirlene Zardin Graeff
Author

Cintia Kazuko Tokuhara
Author

Mariana Liessa R Sanches
Author

Rodrigo Cardoso de Oliveira
Author

# *Annexes*

**ANNEX A** – Manuscript submission letter confirmation from JAOS

## Journal of Applied Oral Science - Manuscript ID JAOS-2018-0329

1 mensagem

**Journal of Applied Oral Science** <onbehalfof@manuscriptcentral.com> 3 de junho de 2018 23:01

Responder a: jaos@usp.br
Para: rodrigocardoso@usp.br
Cc: mszgraef@usp.br, cintia.tokuhara@usp.br, rodrigocardoso@usp.br

03-Jun-2018

Dear Dr. Oliveira:

Your manuscript entitled "On a novel method for evaluation of the mineralization process of osteoblasts on biomaterials surfaces" has been successfully submitted online and is presently being given full consideration for publication in the Journal of Applied Oral Science.

Your manuscript ID is JAOS-2018-0329.

Please mention the above manuscript ID in all future correspondence or when calling the office for questions. If there are any changes in your street address or e-mail address, please log in to ScholarOne Manuscripts at https://mc04.manuscriptcentral.com/jaos-scielo and edit your user information as appropriate.

You can also view the status of your manuscript at any time by checking your Author Center after logging in to https://mc04.manuscriptcentral.com/jaos-scielo.

WARNING: From July, 1st, 2015 SciELO Brasil will adopt Creative Commons license CC-BY:

"This license lets others distribute, remix, tweak, and build upon your work, even commercially, as long as they credit you for the original creation. This is the most accommodating of licenses offered. Recommended for maximum dissemination and use of licensed materials."

For more information about this initiative, please access:
http://blog.scielo.org/en/2015/06/19/scielo-adopts-cc-by-as-main-open-access-attribution/

Thank you for submitting your manuscript to the Journal of Applied Oral Science.

Sincerely,
Journal of Applied Oral Science Editorial Office